Economic Geology, v. 102, pp. 585–609

The LaRonde Penna Au-Rich Volcanogenic Massive Sulfide Deposit, Abitibi Greenstone Belt, Quebec: Part I. Geology and Geochronology*

P. Mercier-Langevin,†

Geological Survey of Canada, 490 rue de la Couronne, Québec, QC G1K 9A9, Canada, and Institut national de la recherche scientifique–Centre Eau, Terre et Environnement, 490 rue de la Couronne, Québec, QC G1K 9A9, Canada

B. Dubé,

Geological Survey of Canada, 490 rue de la Couronne, Quebec, Canada G1K 9A9

M. D. Hannington, **

Geological Survey of Canada, 601 Booth Street, Ottawa, Ontario K1A 0E8, Canada

D. W. Davis,

Department of Geology, Earth Sciences Centre, University of Toronto, 22 Russell Street, Toronto, Ontario M5S 3B1, Canada

B. Lafrance,

Ministère des Ressources naturelles et de la Faune, 400 Lamaque Blvd., Val-d'Or, QC J9P 3L4, Canada, and Cogitore Resources, 1300 Saguenay Blvd., Rouyn-Noranda, QC J9X 7C3, Canada

and G. Gosselin

Agnico-Eagle Mines Ltd, Exploration Division, Val-d'Or, Québec J9P 4N9, Canada

Abstract

The LaRonde Penna Au-rich volcanogenic massive sulfide (VMS) deposit is the largest Au deposit currently mined in Canada (58.8 Mt at 4.31 g/t, containing 8.1 Moz of Au). It is part of the Doyon-Bousquet-LaRonde mining camp located in the eastern part of the Blake River Group of the Abitibi greenstone belt which is host to several of the world's most important, present and past, Au-rich VMS deposits (e.g., Horne, Quemont, Bousquet, Bousquet 2-Dumagami).

The LaRonde Penna deposit consists of massive to semimassive sulfide lenses (Au-Zn-Ag-Cu-Pb), stacked in the upper part of a steeply dipping, south-facing homoclinal volcanic sequence composed of extensive tholeiitic basaltic flows (Hébécourt Formation) overlain by tholeiitic to transitional, mafic to intermediate, effusive and volcaniclastic units at the base (lower member of the Bousquet Formation) and transitional to calc-alkaline, intermediate to felsic, effusive and intrusive rocks on top (upper member of the Bousquet Formation). The mafic to felsic volcanism of the Hébécourt Formation and of the lower member of the Bousquet Formation formed an extensive submarine basement or platform on which the intermediate to felsic rocks of the upper member of the Bousquet Formation were emplaced at restricted submarine eruptive centers or as shallow composite intrusive complexes. The submarine felsic volcanic rocks of the upper member of the Bousquet Formation are characterized by dacitic to rhyodacitic autoclastic (flow breccia) deposits that are cut and overlain by rhyodacitic and rhyolitic domes and/or partly extrusive cryptodomes and by intermediate to mafic sills and dikes.

This volcanic architecture is thought to have been responsible for internal variations in ore and alteration styles, not only from one lens to another, but also along a single mineralized horizon or lens. In the upper part of the mine, the 20 North lens comprises a transposed pyrite-chalcopyrite (Au-Cu) stockwork (20N Au zone) overlain by a pyrite-sphalerite-galena-chalcopyrite-pyrrhotite (Zn-Ag-Pb) massive sulfide lens (20N Zn zone). The latter was formed, at least in part, by replacement of footwall rhyodacitic autoclastic deposits emplaced within a subbasin located between two rhyolite domes or cryptodomes. The 20N Zn zone tapers with depth in the mine and gives way to the 20N Au zone. At depth in the mine, the 20N Au zone consists of semimassive sulfides (Au-rich pyrite and chalcopyrite) enclosed by a large aluminous alteration halo on the margin of a large rhyolitic dome or cryptodome.

U-Pb zircon geochronology gives ages of 2698.3 ± 0.8 and 2697.8 ± 1 Ma for the footwall and hanging-wall units of the 20 North lens, respectively. Thus, the formation of the 20 North lens was coeval with other VMS deposits in the Bousquet Formation and in the uppermost units of the Blake River Group. Although deformation and metamorphism have affected the primary mineral assemblages and the original geometry of the deposit, these events were not responsible for the different auriferous ore zones and alteration at LaRonde

† Corresponding author: e-mail, pmercier@nrcan.gc.ca
*Geological Survey of Canada contribution 20060352
**Present address: University of Ottawa, 140 Louis Pasteur, Ottawa, Ontario, Canada K1N 6N5.

Penna. Studies of the LaRonde Penna deposit show that the hydrothermal system evolved in time and space from near-neutral seawater-dominated hydrothermal fluids, responsible for Au-Cu-Zn-Ag-Pb mineralization, to highly acidic fluids with possible direct magmatic contributions, responsible for Au ± Cu-rich ore and aluminous alteration. The different ore types and alteration reflect the evolving local volcanic setting described in this study.

Introduction

The LaRonde Penna deposit (Agnico-Eagle Mines Ltd.) is an Au-rich volcanogenic massive sulfide (VMS) orebody composed of stacked semimassive to massive sulfide lenses in a south-facing homoclinal volcanic sequence. The deposit contains reserves and geologic resources (February 2006) of 46.5 million tons (Mt) of ore or 6.7 million ounces (Moz) of Au, at an average grade of 4.51 g/t Au, 2.04 percent Zn, 0.34 percent Cu, and 42.7 g/t Ag. Between 2000 and 2005, 12.3 Mt of ore at 3.53 g/t Au (1.4 Moz of Au), 2.66 percent Zn, 0.29 percent Cu, and 53.7 g/t Ag were extracted from the LaRonde Penna mine (Table 1). The main ore lens is about 500 m wide, at least 2,300 m long (vertical extent), and locally up to 40 m thick. The deposit is located in the eastern part of the Blake River Group (Fig. 1) and is part of the Doyon-Bousquet-LaRonde mining camp, one of the major Au districts of the prolific Archean Abitibi greenstone belt.

The host sequences of Au-rich VMS deposits worldwide are characterized by either effusive volcanic, volcaniclastic, or epiclastic mafic to felsic rocks, and mixed volcanogenic sedimentary sequences that include terrigenous, pelagic, or chemical sedimentary rocks. In most cases, the felsic rocks are dacitic to rhyodacitic in composition and are characterized by a transitional to low K calc-alkaline magmatic affinity typical of the fractionated magmas formed in volcanic arcs or rifted back arcs (Huston, 2000; Hannington et al., 1999). Barrie and Hannington (1999) and Hannington et al. (1999) noted a much higher proportion of felsic volcanic rocks versus mafic volcanic rocks in the volcanic successions that host Au-rich VMS.

Although there are several good general reviews of Au-rich VMS (e.g., Hannington and Scott, 1989; Huston and Large, 1989; Huston et al., 1992; Large, 1992; Poulsen and Hannington, 1995; Sillitoe et al., 1996; Hannington et al., 1999; Huston, 2000), detailed descriptions are limited, and many of the geologic parameters considered critical for ore formation remain speculative. The LaRonde Penna mine represents an opportunity to describe the geology of a world-class Au-rich volcanogenic sulfide deposit.

Previous studies of the deposits of the Doyon-Bousquet-LaRonde mining camp were hindered by the deformation that has affected all of the deposits and by the lack of preserved primary features (e.g., Tourigny et al., 1989a). This led some authors to conclude that all or part of the Au present in the VMS deposits of the district had been structurally introduced during the main regional deformation event, some 15 m.y. after the formation of the VMS deposits (e.g., Tourigny et al., 1989b, 1993; Marquis et al., 1990b). However, the discovery of the LaRonde Penna deposit by Agnico-Eagle Mines Ltd. in a less deformed part of the volcanic sequence provided a unique opportunity to examine the primary features and the genesis of a Au-rich VMS deposit more closely.

In this paper, the stratigraphic, geochronologic, and structural context of the deposit are presented to establish the primary setting of the ore lenses. Two other papers (Dubé et al., 2007; Mercier-Langevin et al., 2007) address the nature of the hydrothermal alteration, the primary lithogeochemistry and petrogenesis of the volcanic rocks, and the mineralogy and geochemistry of the ore zones and alteration, which together contribute to the understanding of the origin of Au-rich VMS in the district.

Regional Geologic Setting

Rocks of the mine sequence in the Doyon-Bousquet-LaRonde mining camp are part of the upper part of the 2703 to 2694 Ma Blake River Group (Péloquin et al., 1990; Barrie et al., 1993; Mortensen, 1993; Ayer et al., 2002; Lafrance et al., 2005). Lafrance et al. (2003) divided the sequence into the Hébécourt Formation in the north and the Bousquet Formation in the south (Fig. 1). The Hébécourt Formation is mainly composed of tholeiitic mafic rocks (basalts and gabbro sills) and is overlain by the Bousquet Formation. The volcanic rocks of the Bousquet Formation are characterized by a gradual evolution from tholeiitic at the base (north) to calc-alkaline at the top (south). The Bousquet Formation is further subdivided into a lower member and an upper member. The lower member is composed of tholeiitic to transitional mafic

Table 1. Summary of Production, Reserves, and Geologic Resources for the LaRonde-Bousquet 2 Au-Rich VMS Complex

Mine		Tonnage	Au		Ag		Cu		Zn	
		(Mt)	(g/t)	(Moz)	(g/t)	(Moz)	(%)	(t)	(%)	(t)
Dumagami	Production (1988-1999)	7.33	6.27	1.48	11.7	2.76	0.47	34,198	0.35	4,994
Bousquet 2	Production (1990-2002)	8.14	8.14	2.13			0.56	45,762		
	Total Dumagami-Bousquet 2	15.47	7.25	3.61	11.7	2.76	0.52	79,959	0.35	4,994
LaRonde Penna	Production (2000-2005)	12.3	3.53	1.39	53.67	21.22	0.29	35,008	2.66	327,217
	Reserves and resources	46.46	4.51	6.74	42.66	63.72	0.34	157,967	2.04	947,801
	Total LaRonde Penna	58.76	4.31	8.13	44.96	84.94	0.33	192,975	2.17	1,275,018
Total LaRonde-Bousquet 2 complex		74.23	4.92	11.74	41.27	87.7	0.37	272,934	1.94	1,280,011

Compiled from mining company annual reports

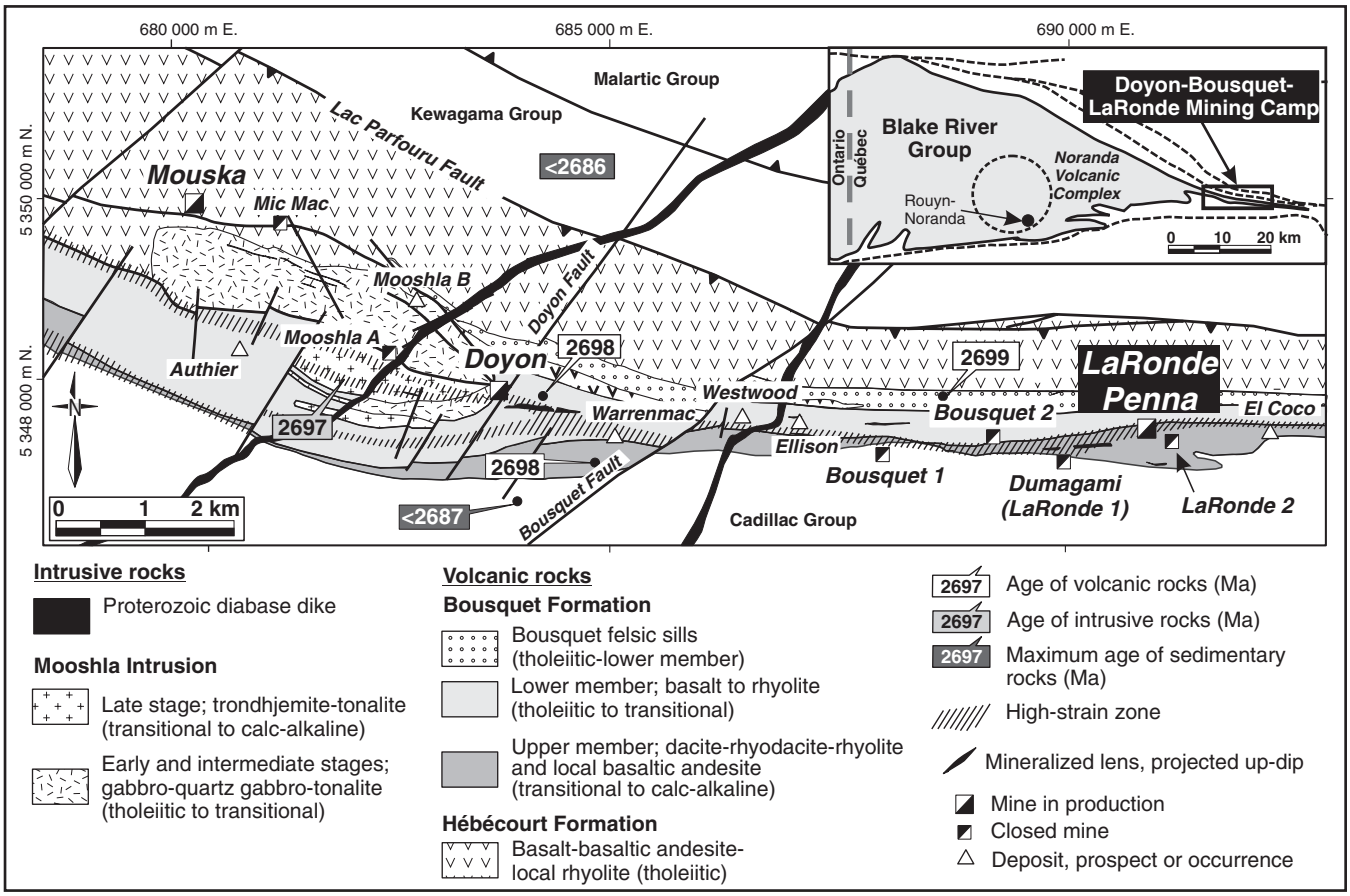

FIG. 1. Simplified geologic map of the Doyon-Bousquet-LaRonde mining camp showing the location of the LaRonde Penna mine and other active and past producing mines relative to the major faults of the area. The location of the Doyon-Bousquet-LaRonde mining camp in the eastern part of the Blake River Group (Bousquet Formation) of the Abitibi subprovince is shown in the inset. Modified from Dubé et al. (2004).

to felsic rocks, whereas the upper member is dominated by transitional to calc-alkaline intermediate to felsic rocks (Lafrance et al., 2003; Mercier-Langevin et al., 2004), defining a continuous magmatic trend. The units of the lower member are laterally extensive, whereas the felsic units of the upper member are laterally restricted and form coalesced flows (Stone, 1990; Lafrance et al., 2003). The lower member of the Bousquet Formation is cut by the synvolcanic Mooshla intrusion in the Doyon mine area west of LaRonde Penna (Fig. 1; Stone, 1990; Lafrance et al., 2003; Galley and Lafrance, 2007). This intrusion hosts parts of the Doyon deposit, which comprises epizonal "intrusion-related" sulfide-rich Au-Cu veins, and parts of the Mouska deposit, which comprises orogenic (or remobilized) sulfide-rich Au-Cu veins (Belkabir and Hubert, 1995; Gosselin, 1998; Galley and Lafrance, 2007).

The area sustained major regional deformation responsible, at least in part, for the present geometry of the camp. The D_1 event caused regional folding of the Blake River Group (Hubert et al., 1984) and was overprinted by D_2, which is the main deformation event in the Doyon-Bousquet-LaRonde area. An east-west–trending, steeply south dipping penetrative schistosity (regional S_2) is present everywhere in the camp and is responsible for strong flattening, stretching, folding, and shearing of the primary features in most deposits (e.g., Bousquet: Tourigny et al., 1989b; Bousquet 2: Tourigny et al., 1993; Dumagami: Marquis et al., 1990b; Doyon: Savoie et al., 1991). A north-northeast–trending cleavage is locally superimposed on the main schistosity and late sinistral north-northeast–trending faults are locally developed. Two episodes of metamorphism have been recognized in the area; a prograde upper greenschist-lower amphibolite facies episode, associated with the main deformation event D_2, and a subsequent retrograde greenschist facies event (Dimroth et al., 1983a, b; Tourigny et al., 1989a; Marquis et al., 1990a; Powell et al., 1995a; Lafrance et al., 2003; Mercier-Langevin, 2005; Dubé et al., 2007).

LaRonde Penna Mine Area

The mineralized lenses of the LaRonde Penna mine are characterized by semimassive to massive sulfide lenses or narrow horizons of transposed sulfide veins and veinlets commonly associated with disseminated sulfides. The lenses are spatially associated with several metamorphosed alteration assemblages developed in both the footwall and the hanging wall, as discussed by Dubé et al. (2007). These lenses are stacked in the upper member of the Bousquet Formation (Fig. 2) on different horizons and represent different episodes of sulfide precipitation in a single protracted hydrothermal

system (Dubé et al., 2004; Mercier-Langevin, 2005). All the lenses are characterized by an Au-Zn-Cu-Ag-Pb polymetallic signature. Most of the ore currently extracted from the LaRonde Penna mine comes from the 20 North and 20 South lenses, which are mined from 800 m to more than 2,300 m below surface (Fig. 2B). These two lenses can be traced to a depth of more than 3,000 m, and the deposit is still open at depth. The 20 North lens, which is the main lens of the deposit, has been subdivided into two zones: the 20N Au zone at the base (north) and the 20N Zn zone on top (south) (Fig. 2B). The 20N Au zone is composed of auriferous pyrite and chalcopyrite veins and veinlets forming a dense stockwork that is now strongly flattened and partially transposed. This Au-rich stockwork is hosted in the upper part of rhyodacitic to rhyolitic flow breccia. The 20N Zn zone forms a massive sulfide lens composed mainly of pyrite, sphalerite, chalcopyrite, and galena. At depth in the mine, the 20N Au zone changes gradually into disseminated to semimassive to locally massive sulfides composed of auriferous pyrite and chalcopyrite hosted in a quartz, kyanite, andalusite, staurolite, and muscovite schist, referred to as the aluminous zone (see Dubé et al., 2007). The 20N Zn zone gradually disappears at depth as the aluminous zone develops. Massive sulfides composed of auriferous pyrite, chalcopyrite, and sphalerite have been intersected in the deepest part of the 20 North lens and suggest the development of a second Au-Cu-Zn-Ag zone associated with the aluminous alteration at depth in the mine.

The 20 South lens is located higher in the stratigraphic sequence and forms a semimassive to massive sulfide lens composed of varying amounts of pyrite, sphalerite, chalcopyrite, galena, and pyrrhotite (Dubé et al., 2004). This lens is thicker (up to 10 m) in the upper levels of the mine and gets thinner with increasing depth.

A number of satellite lenses are found in the LaRonde Penna volcanic succession (LaRonde-Bousquet 2 Au-rich VMS complex; Table 1). Zone 5 (Dumagami mine) is the upper half of the massive sulfide lens mined at greater depth from the Bousquet 2 mine (Marquis et al., 1990a; Tourigny et al., 1993). Zones 6 and 7 were mined to surface (LaRonde shaft 2) and can be traced to a depth of more than 2,300 m, with zone 7 currently being mined at depth from the LaRonde Penna shaft. These zones are composed of semimassive to massive pyrite, chalcopyrite, and sphalerite forming narrow lenses. An andesitic to dacitic talus breccia containing Au-rich massive sulfide clasts at the margin of zone 6 has been mined close to surface from shaft 2.

Stratigraphic Units Hosting the LaRonde Penna Deposit

The LaRonde Penna Au-rich massive sulfide lenses were emplaced within a complex volcanic environment, and the major rock units described locally show remarkably well preserved primary features, despite the intensity of metamorphism and deformation (north-south shortening) that significantly modified the aspect ratios of features in the area. The LaRonde Penna deposit is entirely hosted in the upper member of the Bousquet Formation (Fig. 2), and these rocks are the focus of the present study. The main characteristics of each unit of the upper member of the Bousquet Formation at LaRonde Penna are summarized in Table 2. A detailed geochemical and petrogenetic study of the LaRonde Penna volcanic units is presented in the companion paper by Mercier-Langevin et al. (2007a).

Hébécourt Formation

The Hébécourt Formation constitutes the base of the volcanic sequence hosting the LaRonde Penna deposit. It is in structural contact with the underlying younger sedimentary rocks of the Kewagama Group (ca. 2686 Ma: Davis, 2002) along the Lac Parfouru fault (Fig. 1). The present thickness varies from about 1,000 to 1,200 m immediately north of the LaRonde Penna mine. It consists of thick, massive to pillowed tholeiitic andesitic to basaltic flow units (Fig. 2A). Some of these are characterized by highly variolitic to amygdaloidal pillows (Fig. 3A). Numerous fine-grained gabbroic sills cut the basalts. Rocks are characterized by a granoblastic texture and are composed of various amounts of hornblende, chlorite, biotite, feldspar, sericite, and epidote. This formation was emplaced as subaqueous flows, either in the setting of a basalt plane (Dimroth et al., 1982; Lafrance et al., 2003) or a shield volcano (Stone, 1990).

Bousquet Formation, lower member

Four different units characterize the lower member of the Bousquet Formation at LaRonde Penna. From north (base) to south (top), these are the Bousquet felsic sill complex (unit 2.0), the Sphynx volcaniclastic unit (unit 3.2), the Bousquet scoriaceous tuffs (unit 3.3) and the Bousquet heterogeneous unit (unit 4.4). The lower member is now between 150 and 300 m thick in the LaRonde Penna area and is thinner than elsewhere in the Doyon-Bousquet-LaRonde mining camp.

The felsic sill complex (unit 2.0) is composed of quartz- and feldspar-phyric, tholeiitic, rhyolitic sills intruding the Hébécourt Formation (Fig. 2A). These sills are characterized by up to 35 vol percent blue quartz microphenocrysts ($\leq$2 mm) and angular feldspar phenocrysts (1–2 mm) in a sericitized matrix. The Sphynx volcaniclastic unit (unit 3.2) is composed of fragmental feldspar-phyric basalt and/or andesite characterized by a fine-grained matrix of chlorite, epidote, carbonate, and sericite. The scoriaceous tuffs (unit 3.3, Fig. 2A) are mainly composed of highly altered tholeiitic andesitic to dacitic blocks and lapilli tuffs (Fig. 3B) dominated by scoriaceous fragments in which vesicularity varies from 20 to 40 vol percent. The amygdules are typically 1 to 2 mm in diameter and are filled by epidote and carbonate and, in some cases, by quartz and feldspar. The morphology of this unit suggests either a pyroclastic origin (Stone, 1990) or an autoclastic origin (e.g., coalescent subaqueous lava fountain deposits: Lafrance et al., 2003). The last unit of the lower member (heterogeneous unit 4.4) is mainly exposed underground (Fig. 2). This unit hosts the Bousquet mine zones 4 and 5, and parts of the Westwood, Warrenmac, and Ellison Au ± Cu-Zn-Ag deposits west of LaRonde Penna (see figs. 1 and 3 of Mercier-Langevin et al., 2007b). In the LaRonde Penna mine area, it is more homogeneous and mainly composed of highly altered, glomeroporphyritic, tholeiitic to transitional, massive, pillowed and brecciated (autoclastic) basaltic and andesitic flows (Fig. 2A) in sheared contact with basal units of the upper member of the Bousquet Formation. Rocks of this unit are characterized by abundant feldspar phenocrysts (5–40 vol %) in a fine-grained granoblastic matrix of actinolite, feldspar,

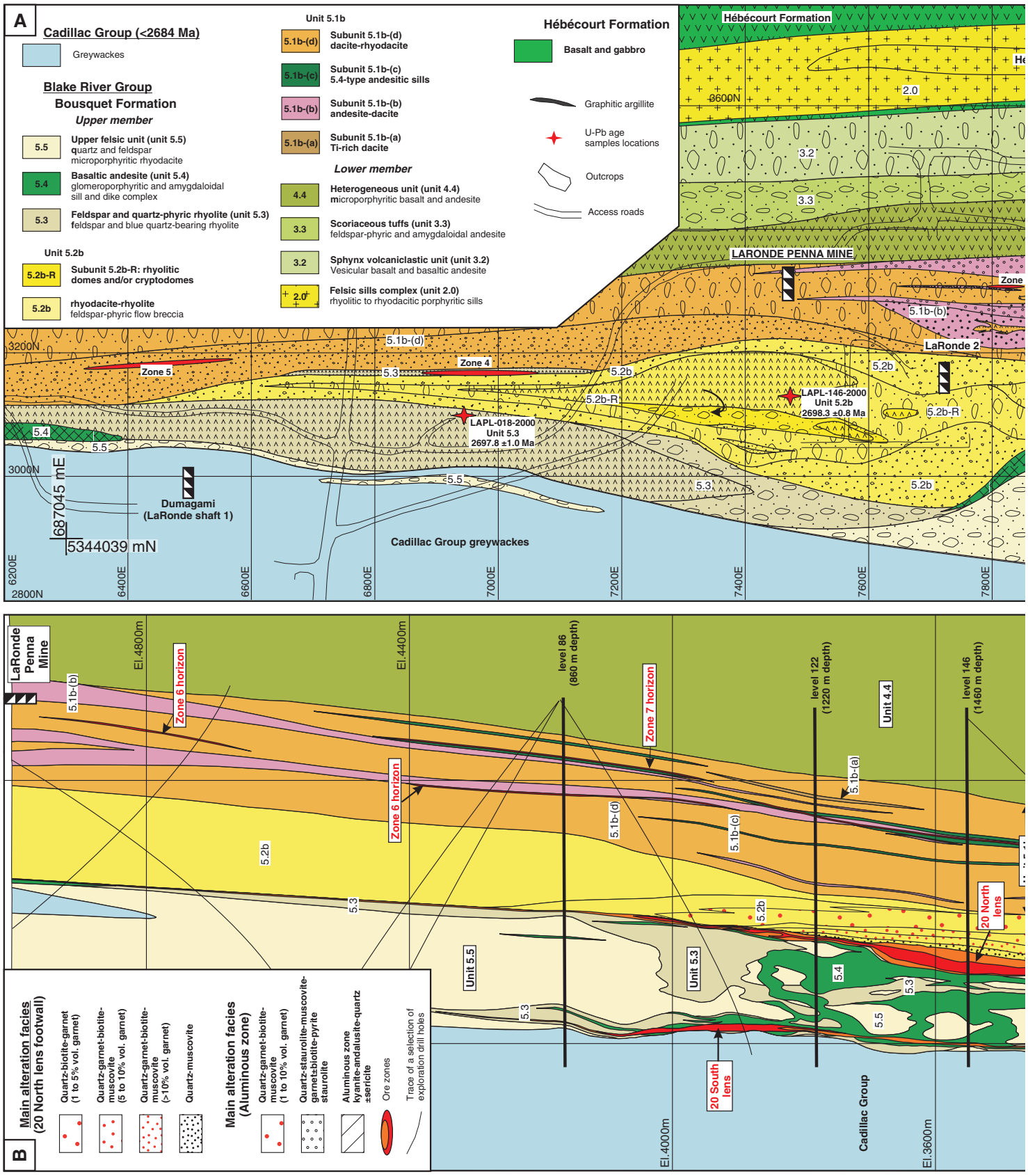

FIG. 2. A. Surface map of the LaRonde Penna mine area showing the distribution of the main units and the main volcanic facies characterizing the section through the central axis of the deposit (section 7880 E on surface) showing the distribution of the upper member of the Bousquet Formation, tion were omitted on this section for clarity.

TABLE 2. Summary of the Main Characteristics of the Units of the Upper Member of the Bousquet Formation that Host the LaRonde Penna Deposit

Lithology	Lithofacies[1]	Inferred volcanic setting
High Ti dacite (subunit 5.1b-(a), tholeiitic)	5- to 25-m-thick feldspar-microporphyritic and amygdaloidal sills with minor volcaniclastics	Intrusive, mostly as shallow sills
Andesite-dacite (subunit 5.1b-(b), transitional)	Massive, pillowed, amygdaloidal, and feldspar-phyritic flows, up to 50 m thick, and hyaloclastite (crystal tuffs) mixed with polymictic volcaniclastic beds; millimeter- to centimeter-scale quartz and carbonate-filled amygdules; ≤10 vol % feldspar microphenocrysts in a recrystallized matrix	Effusive, subaqueous flow and flow breccia with thin beds of volcanogenic sedimentary deposits in depressions
Andesitic sills (subunit 5.1b-(c), transitional)	2- to 10-m-thick feldpar-microporphyritic and amygdaloidal sills emplaced within the dacite-rhyodacite (subunit 5.1b-(d))	Intrusive, mostly as shallow sills
Dacite-rhyodacite (subunit 5.1b-(d), ± calc-alkaline)	25- to 150-m-thick sequence of massive, microporphyritic domes with lobes and flow breccia; 5-15 vol %, 1-2 mm albite-labradorite phenocrysts, 2-15 vol % quartz amygdules, recrystallized volcanic glass (feldspar and quartz matrix)	Effusive, subaqueous flows, domes, lobes, and flow breccia
Rhyodacite-rhyolite (unit 5.2b, ± calc-alkaline)	Mostly feldspar-phyric flow breccia (block and lapilli) with cogenetic domes and lobes, up to 200 m thick; ≤15 vol %, 1-2 mm albite microphenocrysts in a fine-grained, recrystallized quartz and felspar matrix	Effusive, subaqueous flow breccia and domes/lobes
Rhyolitic domes or cryptodomes (subunit 5.2b-R, calc-alkaline)	Massive feldspar-phyric domes and/or cryptodomes, carapace (in situ) breccia and flow breccia (block and lapilli), up to 100 m thick; ≤15 vol %, 1-2 mm albite microphenocrysts and ≤2 vol %, 1 mm quartz microphenocrysts, in a fine-grained, recrystallized quartz and feldspar matrix	Effusive ± intrusive, subaqueous dome and flow breccia complex
Feldspar and quartz-phyric rhyolite (unit 5.3, calc-alkaline)	Massive and brecciated feldspar and quartz-phyric flows, domes, and flow breccia (block and lapilli) with fine-grained volcaniclastics (crystal tuffs); 5-15 vol %, 1-2 mm rounded and partially resorbed blue quartz microphenocrysts and 7 to 15 vol %, 1-2 mm zoned plagioclase microphenocrysts, in a sericitized quartz and feldspar matrix	Intrusive (dikes+sills) and extrusive (domes and volcaniclastic beds)
Basaltic andesite (unit 5.4, transitional)	Massive sills and dikes complex with microporphyritic to glomeroporphyritic facies (base: ≥10 vol %, 1-10 mm zoned plagioclase phenocrysts in a crystalline matrix of feldpsar laths and biotite-hornblende) and fine-grained amygdaloidal facies (top: ≤20 vol %, 1-10 mm coalesced quartz amygdules in a very fine grained matrix)	Intrusive (shallow sill and dike complex)
Upper felsic unit (unit 5.5, calc-alkaline)	Massive domes and flow breccia (block and lapilli) with fine-grained volcaniclastics (crystal tuffs); 5-20 vol % albite microphenocrysts in a recrystallized quartz and feldspar matrix	Effusive (domes and flow breccia)

[1] Present thickness indicated

epidote, chlorite, quartz, carbonate, biotite, sericite, leucoxene, and pyrite.

Bousquet Formation, upper member

The upper member of the Bousquet Formation is thicker at LaRonde Penna than elsewhere in the Doyon-Bousquet-LaRonde mining camp, varying from 285 to 500 m. In its thickest part, it contains all the sulfide lenses of the LaRonde Penna mine and the Bousquet 2-Dumagami deposit. The upper member is composed of five main stratigraphic units described here from north (base) to south (top).

Dacite-rhyodacite (unit 5.1b): The dacite-rhyodacite has been divided into four sub-units in the LaRonde Penna area based on petrographic and geochemical characteristics (see also Mercier-Langevin et al., 2007a). The main subunit (5.1b-(d)) is composed of transitional to calc-alkaline dacitic to rhyolitic volcanic-volcaniclastic rocks intercalated with intermediate massive and volcaniclastic deposits (subunit 5.1b-(b)). Two types of mafic to intermediate sills (subunits 5.1b-(a) and -(c)), a few meters in thickness, were emplaced within the dacitic to rhyodacitic deposits. These four subunits form a pile that is now 100 to 300 m thick in the footwall sequence of the LaRonde Penna mine (Fig. 2A).

The dacite-rhyodacite subunit (5.1b-(d); Fig. 2A and Table 2) forms small domes and lobes, a few meters to a few tens of meters wide, surrounded by homogeneous, extensive autoclastic (flow breccia) deposits (Fig. 3C). Some were emplaced, at least in part, on the sea floor and are associated with restricted heterolithic talus breccia deposits composed of felsic fragments mixed with some andesitic fragments and Au-rich sulfide clasts (Fig. 3D) related to the zone 6 Au-Cu-Ag-Zn lens. The presence of highly irregular peperitic margins and chilled margins around some of these domes and lobes suggests a subsea-floor emplacement (McBirney, 1963; McPhie and Allen, 1992). The autoclastic felsic deposits are texturally variable, ranging from proximal blocky, clast-supported deposits to distal, matrix-supported and lapilli-sized flow-breccia deposits.

The second subunit (5.1b-(b); Table 2) is composed of transitional, intermediate (andesite) to felsic (dacite) flows and

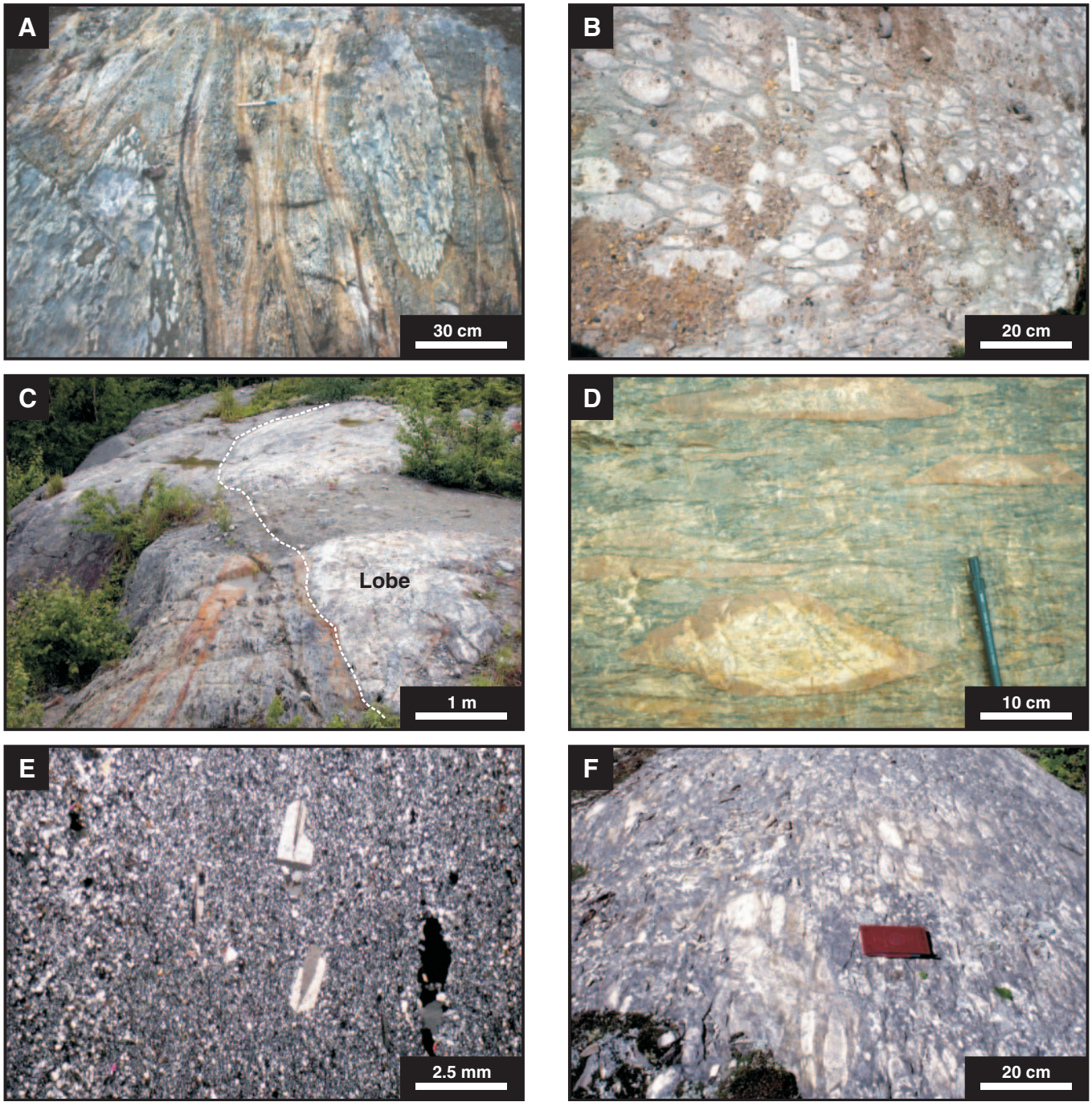

FIG. 3. A. Flattened, pillowed and variolitic basalts of the Hébécourt Formation, northeast of the LaRonde Penna mine. B. Scoriaceous tuff (unit 3.3) of the lower member of the Bousquet Formation, northeast of the LaRonde Penna mine. C. Subunit 5.1b-(d) dacite-rhyodacite lobe intruding andesite-dacite fine-grained hyaloclastite of subunit 5.1b-(b). D. Example of the coarse talus breccia of subunit 5.1b-(b) seen on surface near zone 6 where Au-rich massive sulfide clasts were concentrated and mined economically. E. Example of well-preserved dacite-rhyodacite feldspar microporphyritic volcanic rocks of subunit 5.2b. F. Rhyolitic carapace breccia (in situ hyaloclastite) located on top of the 20 North lens footwall dome and/or cryptodome exposed on surface (part of unit 5.2b).

volcaniclastic rocks. It is intercalated with dacite-rhyodacite (subunit 5.1b-(d)) (Fig. 2). Fine-grained hyaloclastites are locally developed on top of the andesitic flows. These hyaloclastites have the same composition as the flows and are composed of broken feldspar crystals in a highly altered, fine-grained matrix. In outcrop, the andesitic flows and hyaloclastites are locally spatially associated with thin graphitic argillite horizons that represent interflow, volcanic-derived sedimentation (Fig. 2A).

The third (5.1b-(a)) and fourth (5.1b-(c)) subunits are represented by two different types of feldspar-phyric volcanic rocks (Table 2) that are differentiated mainly by their

geochemical signature (Zr, TiO_2, and SiO_2: see Mercier-Langevin et al., 2007a). These form relatively narrow but extensive sills, locally spatially related to the zones 6 and 7 ore lenses at depth (Fig. 2B). They are generally highly altered owing to their close spatial association with the ore zones.

Rhyodacite-rhyolite (unit 5.2b): The rhyodacite-rhyolite comprises the footwall unit of the 20 North lens at depth (Fig. 2B). Its maximum thickness, about 230 m, is centered in the Penna shaft section (Fig. 2A). Two subunits have been defined based on volcanic facies (Table 2) and geochemical signatures (Mercier-Langevin et al., 2007a). These are volcaniclastic (flow breccia) rhyodacite and massive to brecciated rhyolite intercalated with the volcaniclastic rhyodacitic deposits as domes and/or cryptodomes. Primary textures, including relict perlitic fractures and fine glass shards, are present but are progressively obliterated by the hydrothermal alteration when approaching the 20 North lens at depth.

The massive to brecciated rhyolites are characterized by different volcanic facies typical of felsic domes and partly extrusive cryptodomes (Mercier-Langevin, 2005). Two domes or cryptodomes have been defined in the LaRonde Penna deposit area (Fig. 4). One is exposed on surface (Fig. 2A) and has been mapped in detail (Mercier-Langevin, 2005). It is characterized by a massive core overlain by a carapace breccia or coarse, in situ hyaloclastite (Figs. 2, 3F, 5A). The upper part is characterized by millimeter- to meter-wide flow-banding in which only albite microphenocrysts were preserved from the early diagenetic-hydrothermal alteration of glassy material (cf. Goto and McPhie, 1998; Gifkin and Allen, 2001). The overlying carapace breccia is cut by meter-wide lobes of the cogenetic dome (Fig. 5B). Concentric flow banding can still be recognized in some of these lobes and the presence of flow banding at a high angle to the margins (Fig. 5C) suggests lobe fragmentation, possibly due to slope instability induced by endogenous growth of the dome or cryptodome. This carapace breccia can still be recognized on level 86 (860 m depth; Fig. 5D) and can be traced using geochemistry to a maximum depth of 1,500 m (Fig. 4), where only some breccia clasts are preserved at the base of the 20 North lens (Fig. 5E). The second rhyolite dome or cryptodome has been partially delimited underground (Figs. 2B, 4) using geochemistry; however, hydrothermal alteration precludes the recognition of volcanic facies in this part of the stratigraphy. Some accidental fragments of an equigranular quartz, feldspar, and biotite intrusive rock have been found on the surface within the unit 5.2b flow breccia (Fig. 5F).

The two domes or cryptodomes of unit 5.2b are part of the 20 North lens footwall and show the same overall distribution and attitude as the ore lens (Fig. 4). As discussed below, their geometry is thought to be a key factor in the distribution and the styles of the ore lenses.

Feldspar- and quartz-phyric rhyolite (unit 5.3): This calc-alkaline unit (Mercier-Langevin et al., 2007a), emplaced on top of unit 5.2b, is mostly restricted to the immediate LaRonde Penna and Bousquet 2 area. At LaRonde Penna, it comprises a part of the stratigraphic hanging wall of the 20 North lens and a part of the stratigraphic footwall of the 20 South lens (Fig. 2). Locally, it is intercalated with the upper felsic unit (unit 5.5). Three different volcanic facies characterize this feldspar- and quartz-phyric unit (Table 2): massive,

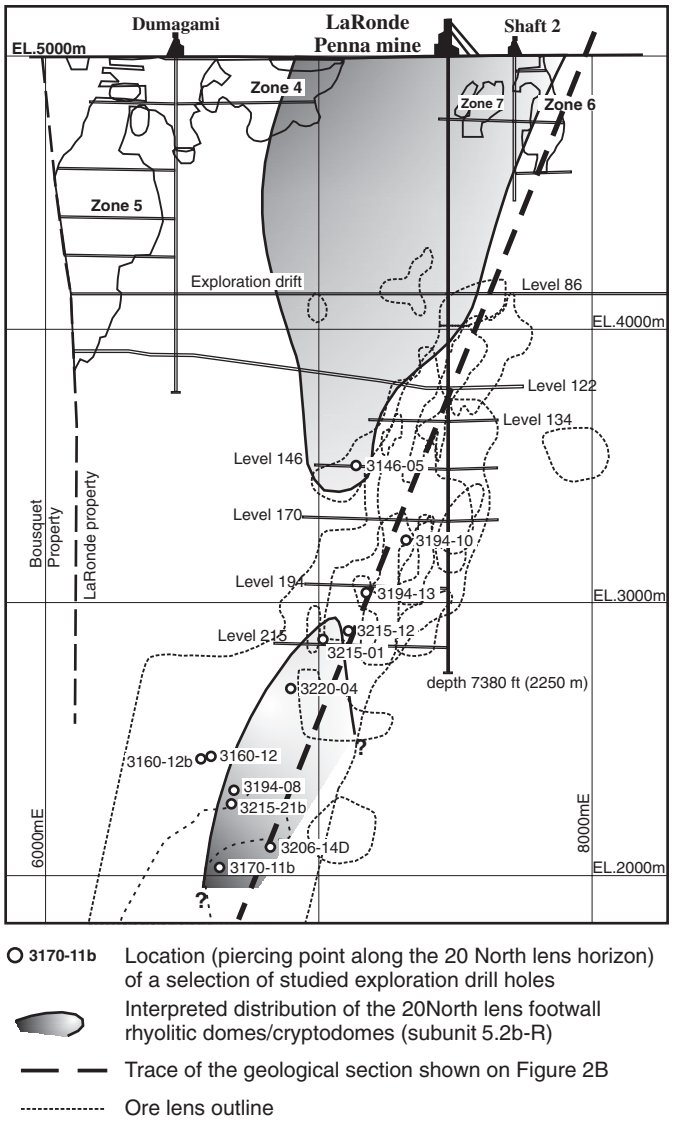

FIG. 4. Composite longitudinal view of the ore lenses of the LaRonde Penna deposit (outline) showing the distribution of the 20 North lens footwall rhyolitic domes or cryptodomes of unit 5.2b (subunit 5.2b-R).

autoclastic, and tuffaceous. The massive part is dominant and is developed from surface to a depth of about 1,500 m between the two main ore lenses (Fig. 2B). Locally, it contains fragments of the underlying unit 5.2b and fragments of the host unit 5.5. The autoclastic facies is developed locally on top of the massive facies near the 20 South lens horizon (Fig. 6B) and may represent a carapace breccia or part of a brecciated flow. The tuffaceous facies is seen toward the west, between the LaRonde Penna and Bousquet 2-Dumagami areas. This facies forms narrow bands of locally laminated and graded beds of crystal-rich tuff intercalated with narrow lenses of graphitic argillite related to unit 5.5 (upper felsic unit).

The feldspar- and quartz-phyric rhyolite (unit 5.3) was probably emplaced as a high-viscosity flow (dome) associated with restricted pyroclastic flows. However, the unit has an irregular distribution (Fig. 2B) and it is largely hosted by the upper felsic unit (5.5), suggesting that it was, at least in part,

FIG. 5. A. In situ fragmentation of the dome-cryptodome rhyolite. B. Rhyolitic lobes intruding the carapace or in situ breccia formed on top of the dome-cryptodome suggesting repeated magmatic pulses. C. Truncated flow-banding texture along the lobe margins. D. Example of unit 5.2b rhyolitic carapace breccia exposed underground in the 20 North lens footwall on level 86 (860 m depth). E. Preserved rhyodacite breccia clast of unit 5.2b in the 20 North lens footwall on level 146 (1,460 m depth). F. Accidental fragment of an equigranular quartz, feldspar, and biotite intrusive rock found in unit 5.2b flow breccia south of the LaRonde Penna mine.

emplaced as an intrusive body (cryptodome) associated with compositionally similar sills and dikes centered in the LaRonde Penna mine area.

Basaltic andesite (unit 5.4): This unit constitutes an important part of the 20 North lens hanging wall and hosts part of the 20 South lens (Fig. 2). It is mainly exposed underground and only in a few outcrops on surface. Its geochemistry is distinct from that of the other units of the upper member of the Bousquet Formation (see Mercier-Langevin et al., 2007a). It comprises a massive sill-dike complex and a few narrow glomeroporphyritic sills that are only very locally developed (Table 2). The sill and dike complex is characterized by a major

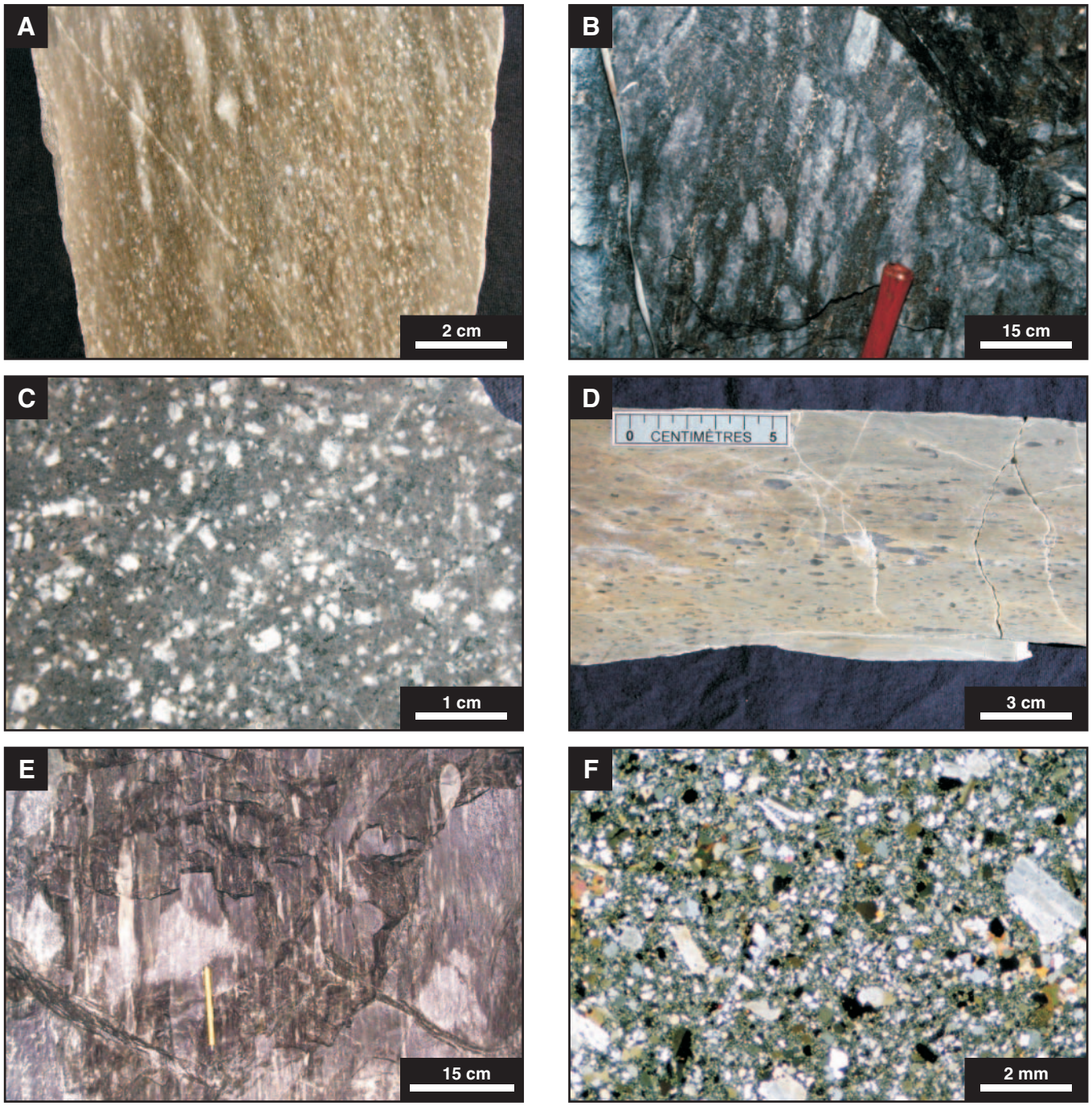

FIG. 6. A. Unit 5.3 feldspar- and quartz-phyric rhyolite characterized by blue-gray quartz microphenocrysts and zoned feldspar microphenocrysts in a sericitized matrix. B. Example from level 122 (1,220 m depth) of the brecciated facies of unit 5.3 (feldspar- and quartz-phyric rhyolite) that characterizes the upper part of the unit in the 20 South lens footwall. C. Basaltic andesite glomeroporphyritic facies of Unit 5.4 that characterizes the lower part of the sill and dike complex located between the 20 North and 20 South lenses. D. Basaltic andesite fine-grained and amygdaloidal facies of Unit 5.4 that characterizes the uppermost part of the sill and dike complex near the 20 South lens in the upper part of the host sequence of the LaRonde Penna deposit. E. Felsic flow breccia deposits of unit 5.5 (upper felsic unit) on level 106 (1,060 m depth) in the 20 South lens footwall close to the contact with the Cadillac Group sedimentary rocks. F. Upper felsic tuffaceous facies of Unit 5.5 characterized by feldspar ± quartz crystal angular fragments in a fine-grained quartzofeldspathic matrix.

feldspar-phyric facies (Fig. 6C) and by a fine-grained amygdaloidal facies that defines the uppermost part of the unit (Fig. 6D).

On surface, the basaltic andesite (unit 5.4) forms two small lenses (Fig. 2A) associated with narrow beds of argillite within the upper felsic unit (unit 5.5, see below). At depth, the

basaltic andesite is thicker and spatially related to the ore lenses (20 North and 20 South), especially in the upper levels of the mine (Fig. 2B). It cuts through the feldspar- and quartz-phyric rhyolite (unit 5.3) and the upper felsic unit (unit 5.5) as shown on Figures 2 and 7 (level 170, 1,700 m depth). The contacts between the basaltic andesite and the felsic rocks are sharp and the basaltic andesite locally contains small felsic fragments. In the deeper parts of the mine, it is present only in the footwall of the 20 South lens (Fig. 2B). It is absent from the hanging wall of the 20 North lens at depth.

The complex distribution, crosscutting relationship with enclosing felsic rocks, and the textures of this unit confirm an intrusive origin. It is mostly discordant to and entirely enclosed within the upper felsic unit (unit 5.5). The concentration of amygdules in the fine-grained matrix in the uppermost part of the complex is interpreted to reflect segregation of volatiles and the formation of a chilled margin on top of the shallow intrusive complex, as is commonly observed in hypabyssal sills (e.g., Branney and Suthren, 1988; McPhie et al., 1993); this indicates that the stratigraphic top is to the south.

Upper felsic unit (unit 5.5): This unit comprises rhyodacitic to rhyolitic volcanic rocks. Its composition is similar to that of units 5.1b, 5.2b, and 5.3. It consists of thick deposits of fine- to coarse-grained autoclastic material (Fig. 6E) associated with small lobes and some thin intervals of crystal tuffs (Fig. 6F). The autoclastic deposits are composed of block- and lapilli-sized fragments in a fine-grained matrix of the same composition, suggesting emplacement as flow breccia. The upper felsic unit is similar to the rhyodacite-rhyolite flow-breccia deposits of unit 5.2. In outcrop, some isolated fragments of feldspar- and quartz-phyric rhyolite (unit 5.3) are locally present within the upper felsic unit. The crystal tuffs of unit 5.5 are located in the western part of the map area and are associated with unit 5.3 crystal tuffs and thin argillite beds located between the LaRonde Penna and Bousquet 2-Dumagami deposits.

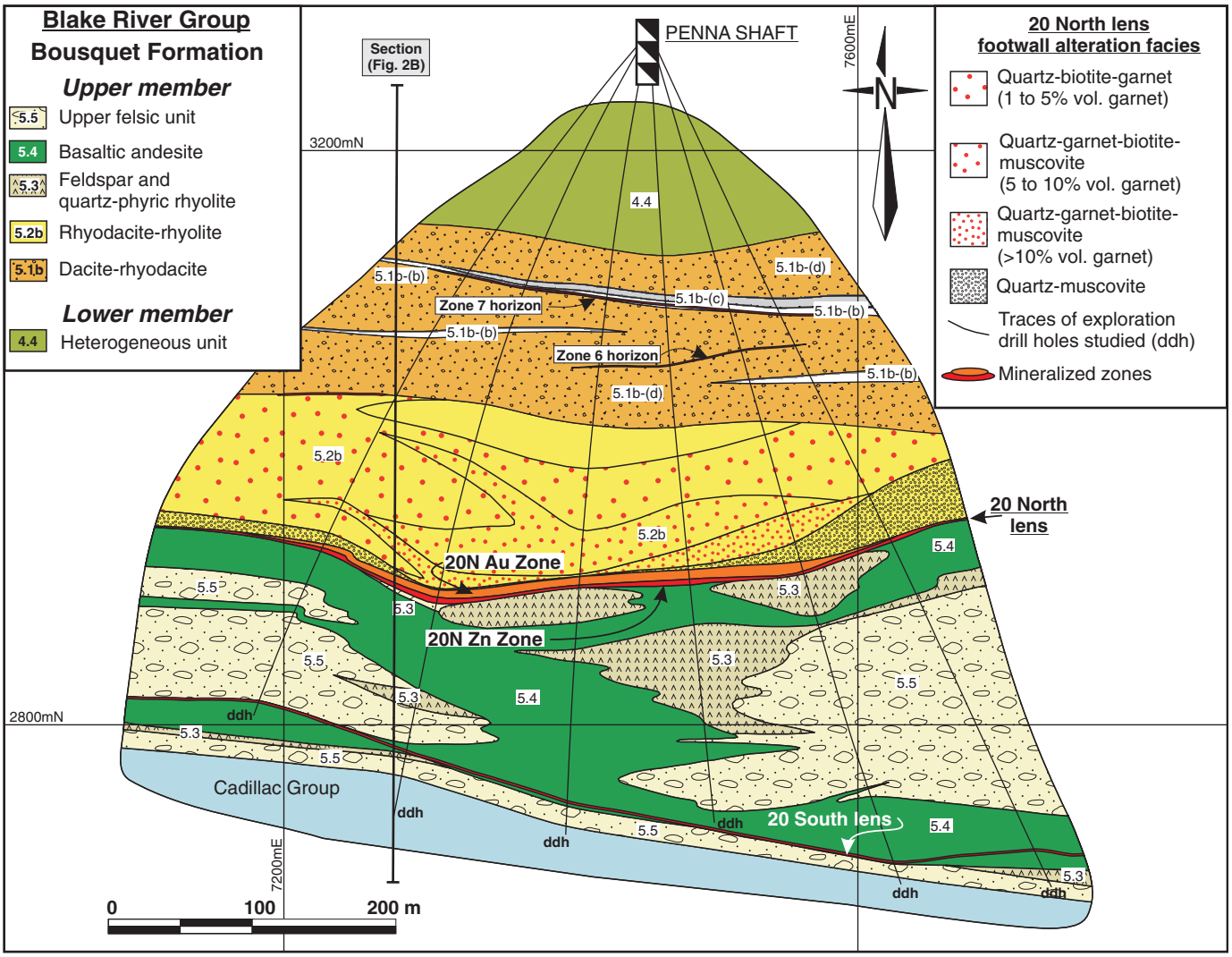

FIG. 7. Geologic map of level 170 (1,700 m depth) showing the distribution of the units of the upper member of the Bousquet Formation and the LaRonde Penna ore lenses and main alteration zones. This map illustrates the complex distribution of the units in the 20 North lens hanging wall and 20 South lens footwall with units 5.3 (feldspar- and quartz-phyric rhyolite) and unit 5.4 (basaltic andesite) emplaced as cryptodome and sill and dike complexes, respectively, within the upper felsic unit (unit 5.5).

Cadillac Group sedimentary rocks

The volcanic host sequence of the LaRonde Penna deposit (Bousquet Formation) is overlain to the south by sedimentary strata of the Cadillac Group (Fig. 2). The Cadillac Group has been described by Dimroth et al. (1982), Lajoie and Ludden (1984), Stone (1990) and Davis (2002), who interpreted it as a turbiditic sequence younger than 2687 Ma. The contact between the volcanic and sedimentary rocks is not exposed on surface in the LaRonde Penna area but it has been intersected in many drill holes and in a few stopes. Regionally this contact has been interpreted both as a major deformation corridor (Dumagami fault of Tourigny et al., 1988, 1989b, 1993; Marquis et al., 1990a) and as a comformable contact (Valliant and Hutchinson, 1982; Stone, 1990). In the LaRonde Penna mine area, the contact is slightly discordant (i.e., erosional) to subconcordant as illustrated in section (Fig. 2B) and in plan view (Figs. 2A, 7).

A thin horizon (<20 cm) of semimassive to massive pyrrhotite and pyrite is commonly present at or near the contact between the volcanic and sedimentary rocks. This sulfide-rich interval at or very near the contact between the Blake River Group volcanic sequence and the Cadillac Group sedimentary sequence may result from expulsion of late hydrothermal fluids and mixing with seawater during a period of nondeposition along the unconformity (Dubé et al., 2004; Mercier-Langevin, 2005).

U-Pb Geochronology of the LaRonde Penna Mine Area

In order to better constrain the timing of formation of the LaRonde Penna deposit, a series of three samples from the upper member of the Bousquet Formation in the mine area was selected for zircon U-Pb geochronology. Detrital zircons from the Cadillac Group sedimentary rocks were also analyzed to help establish the temporal and stratigraphic relationship between volcanism of the Bousquet Formation and sedimentation of the Cadillac Group graywacke in the LaRonde Penna deposit areas. U-Pb isotope determinations were performed at the Royal Ontario Museum. Sample processing, U-Pb isotope analysis, and data reduction followed standard procedures practiced at the Jack Satterly Geochronology Laboratory (Davis and Lin, 2003).

Samples weighed about 15 kg each. Their provenance is given in Table 3. Results of isotopic measurements on zircon, titanite, and rutile (errors are at 2σ) are also listed and plotted in Figure 8. Age calculations were made using the method of Davis (1982) and errors in the text and figures are quoted at the 95 percent confidence level. Error ellipses in Figure 8 are given at the 2σ level.

Results

LAPL-146-2000, rhyodacite-rhyolite (unit 5.2b; Fig. 2A): Sample LAPL-146-2000 is from the 20 North lens footwall unit and was collected on surface south of the LaRonde Penna shaft. The sample contained colorless to brownish prismatic zircons. Five single zircon crystals were analyzed. Four gave overlapping concordant results, the average $^{207}Pb/^{206}Pb$ values of which define an age of crystallization of 2698.3 ± 0.8 Ma for this unit (Fig. 8A). The fifth zircon gave a concordant datum with an inherited age of 2721 ± 3 Ma, probably reflecting derivation from the underlying basement.

LAPL-018-2000, feldspar- and quartz-phyric rhyolite (unit 5.3; Fig. 2A): Sample LAPL-018-2000 is from the 20 North lens hanging-wall unit and was collected on surface west-southwest of the LaRonde Penna shaft. The sample contained colorless to brownish prismatic zircons. Some crystals appeared to contain older cores and were not considered for analysis. Four euhedral zircons gave overlapping, near-concordant results with an average $^{207}Pb/^{206}Pb$ age of 2697.8 ± 1 Ma. The four zircon grains chosen for analysis showed all variations in the population including a pale brown grain, a colorless grain, and grains with a gradational zoning from brownish to colorless. Since these are all indistinguishable in age, their mean age probably represents crystallization of unit 5.3 rhyolites (Fig. 8B).

LABD-462-2001, Cadillac Group sedimentary rocks: Sample LABD-462-2001 was selected from drill hole 3194-10, from 597 to 599 m, where it intersects the contact between the Bousquet Formation volcanic rocks and the overlying graywackes of the Cadillac Group. The sample contained many zircons, most of them colorless to brownish in color and generally prismatic in shape. A selection of six grains were analyzed and gave concordant data (Fig. 8C) with a wide range of $^{207}Pb/^{206}Pb$ ages, from 2689 ± 2 to 2817 ± 2 Ma. The youngest grain gives a maximum age (2689 ± 2 Ma) for deposition of the Cadillac Group sediments near the contact with the underlying volcanic rocks of Bousquet Formation in the LaRonde Penna mine area.

LAPL-144-2000, basaltic andesite (unit 5.4; Fig. 2A): Sample LAPL-144-2000 is from the immediate hanging wall of the 20 North lens at 1,460 m depth and was collected in access drift 146-745 on level 146. The sample contained only strongly fractured zircons and therefore could not be analyzed to obtain a precise crystallization age. However, fresh titanite and rutile crystals, which are found to be intergrown and randomly oriented with feldspar crystals, were analyzed. Three analyses of titanite crystals gave overlapping concordant data with an average age of 2622.4 ± 4 Ma (Fig. 8D). These ages suggest that the titanite grew or was reset during a late, relatively high temperature event in the LaRonde Penna mine area that is correlated with the widely recognized ca. 2660 to 2620 Ma pan-Abitibi metamorphic-plutonic-hydrothermal event (Corfu et al., 1989; Jemielita et al., 1990; Vervoot et al., 1993; Hanes et al., 1994; Powell et al., 1995b; Bleeker et al., 1999; Wyman et al., 2002). Three analyses of rutile crystals gave concordant but somewhat disparate results, with ages varying between 2572 ± 3 and 2583 ± 2 Ma (Fig. 8D). The titanite and rutile ages are younger than the events responsible for the formation of orogenic Au deposits along the Abitibi subprovince major fault zones at ~2670 to 2660 Ma.

Interpretation of the age data

The presence of inherited zircons within the 2698 Ma felsic volcanic rocks that host the LaRonde Penna deposit strongly suggests that the Bousquet Formation was deposited on an older crust that included ca. 2721 Ma components. This is the first reported occurrence of inherited zircons in the Blake River Group, and it suggests that the Blake River Group is underlain by an older volcanoplutonic assemblage. This finding is consistent with an earlier proposal by Ayer et

TABLE 3. U-Pb Isotope Age Data of the Host Volcanic and Sedimentary Rocks of the LaRonde Penna Deposit

No.	Description	Wt (mg)	U (ppm)	Th/U	PbCom (pg)	207/204	206/238	2σ	207/235	2σ	207/206 age (Ma)	2σ	% Disc.
LAPL-146-2000, rhyodacite-rhyolite, unit 5.2b (UTM NAD83; 690838 mE, 5347283 mN)													
1	1 Ab zr, eq, brn	0.001	96.4	0.73	0.35	1717.468	0.518476	0.002816	13.21899	0.07322	2697.439	2.012	0.2
2	1 Ab zr, eq, brn	0.001	155.1	0.55	0.48	2002.401	0.521751	0.001738	13.3051	0.0473	2697.764	1.67	–0.4
3	1 Ab zr, eq, plat, clr	0.006	27.7	0.58	0.24	4226.045	0.517825	0.00218	13.21275	0.05714	2698.736	1.926	0.4
4	1 Ab zr, cpr, brn, incl	0.005	81.2	0.69	0.35	7107.306	0.522254	0.001864	13.32726	0.05048	2698.919	1.384	–0.4
5	1 Ab zr, eq, clr	0.001	37.6	0.59	0.27	915.063	0.526702	0.004406	13.62196	0.11474	2721.009	2.504	–0.3
LAPL-018-2000, feldspar and quartz-phyric rhyolite, unit 5.3 (UTM NAD83; 690299 mE, 5347240 mN)													
6	1 Ab zr, cpr, brn-clr	0.006	20.9	1.31	0.63	1245.66	0.517002	0.002644	13.17334	0.06854	2696.428	2.248	0.5
7	1 Ab zr, cpr, brn-clr	0.008	33.8	0.93	0.79	2112.56	0.517905	0.001314	13.20932	0.03586	2698.051	2.08	0.4
8	1 Ab zr, eq, plat, clr	0.004	11.8	0.88	0.54	550.202	0.516499	0.003208	13.1745	0.08344	2698.18	3.312	0.6
9	1 Ab zr, eq, brn	0.002	116.5	0.7	0.41	3549.004	0.518685	0.001394	13.23104	0.03824	2698.281	1.85	0.2
LABD-462-2001, Cadillac Group sedimentary rocks (ddh 3194-10, from 597m to 599m, 7249E, 2769N mine grid)													
10	1 Ab euh zr, clr, melt incl	0.0032	44.3	0.46	0.37	2710.763	0.54642	0.002926	14.98229	0.0809	2816.875	2.278	0.3
11	1 Ab euh zr, brn, eq	0.0024	107.0	0.71	0.38	4441.348	0.53033	0.001628	13.93028	0.04514	2746.55	1.856	0.2
12	1 Ab euh zr, brn, rod incl	0.0022	190.6	0.68	0.58	4417.438	0.51759	0.001256	13.17221	0.03558	2694.409	1.618	0.2
13	1 Ab euh zr, brn, melt incl	0.0019	105.7	0.86	0.31	4018.935	0.516335	0.001892	13.09658	0.05006	2688.905	1.804	0.2
14	1 Ab euh zr, clr, eq	0.0019	44.3	0.66	0.29	1801.604	0.520653	0.003564	13.31221	0.09192	2702.125	2.386	0.0
15	1 Ab euh zr, brn, melt incl	0.0016	203.2	0.63	0.9	2243.031	0.51767	0.001902	13.18545	0.05108	2695.813	1.676	0.3
LAPL-144-2000, basaltic andesite, unit 5.4 (level 146, drift 146-745, 7424E, 2869N mine grid)													
16	2 rutile, moncx, bk	0.06	2.4	0.03	1.2	654.902	0.490875	0.00462	11.60723	0.11008	2572.305	2.794	–0.1
17	6 rutile gr, polycx, bk	0.1	3.3	0.04	1.82	997.353	0.490417	0.002178	11.6182	0.05396	2575.443	1.986	0.1
18	12 rutiles, moncx, bk	0.1	2.4	0.02	1.31	1010.407	0.490747	0.002918	11.68008	0.07092	2583.195	2.08	0.4
19	5 titanite, frag, pleo clr	0.08	4.3	1.87	25.48	84.259	0.498966	0.007412	12.11937	0.21042	2617.048	10.656	0.4
20	6 titanite, frag, green	0.1	4.4	0.51	26.94	99.093	0.500402	0.00636	12.18976	0.17972	2621.902	9.034	0.3
21	7 titanite, frag, pleo green	0.15	8.1	0.87	42.99	156.518	0.500984	0.0017	12.22423	0.05996	2624.667	6.508	0.3

Abbreviations: Ab = abraded, bk = black, brn = brownish, clr = colorless; cpr = prismatic, eq = equant, euh = euhedral, incl = inclusions, moncx = monocrystals, polycx = polycrystals, zr = zircon

Notes: PbCom = common Pb, assuming all has blank isotopic composition; Th/U calculated from radiogenic $^{208}Pb/^{206}Pb$ ratio and $^{207}Pb/^{206}Pb$ age assuming concordance; uranium decay constants are from Jaffey et al. (1971)

% Disc. = percent discordance for the given $^{207}Pb/^{206}Pb$ age

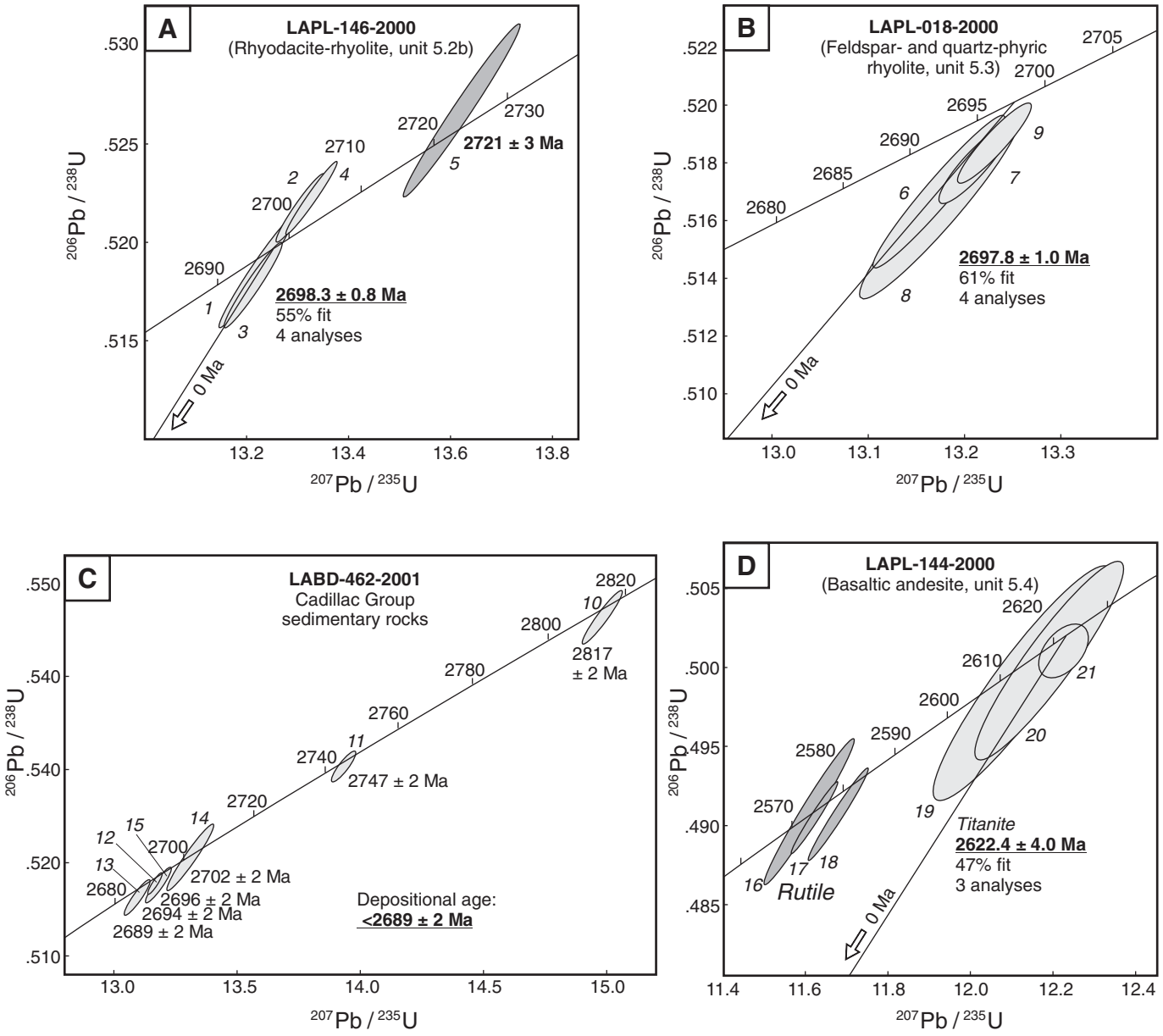

FIG. 8. A. U-Pb concordia diagram for zircons from unit 5.2b (subunit 5.2b-R, rhyolitic domes-cryptodomes; sample LAPL-146-2000). The analytical data are given in Table 3 and sample locations are shown on Figure 2A. B. U-Pb concordia diagram for zircons from unit 5.3 (feldspar- and quartz-phyric rhyolite; sample LAPL-018-2000). The analytical data are given in Table 3 and sample locations are shown on Figure 2A. C. U-Pb Concordia diagram for zircons from Cadillac Group sedimentary rocks (sample LABD-462-2001). The analytical data and sample locations are given in Table 3. D. U-Pb concordia diagram for titanite-rutile crystals from unit 5.4 (basaltic andesite; sample LAPL-144-2000). The analytical data and sample locations are given in Table 3.

al. (2002), who correlated the Blake River Group with the ca. 2700 Ma Skead Group in Ontario, where 2,720 m.y.-old inherited zircons also have been found (Corfu, 1993). These inherited ages are similar to ages of the Hunter Mine Group north of the Destor-Porcupine-Manneville fault zone (Mueller and Mortensen, 2002) as well as the Stoughton-Roquemaure and Kidd-Munro assemblages (Ayer et al., 2002).

Based on the age of the footwall and hanging-wall units of the 20 North lens and the mode of emplacement of the ore in the sequence, the massive sulfide lenses at LaRonde Penna likely have an age close to 2698 Ma. The 20 South lens is, in part, hosted by the feldspar- and quartz-phyric rhyolite (unit 5.3) dated at 2697.8 ± 1 Ma and is therefore the same age or slightly younger than the 20 North lens. A period of erosion and sedimentation followed volcanism, resulting in the formation of an unconformity and deposition of the Cadillac Group graywacke above the Bousquet Formation, both sequences having been later deformed and metamorphosed. The youngest detrital zircon dated in this work is similar in age to the youngest detrital zircons from sedimentary rocks of

the Cadillac and Kewagama groups, sampled in the mine area and about 20 km to the west (2687–2690 Ma: Davis, 2002). This confirms the findings of Davis (2002), who concluded that both turbidite groups were deposited over a short time span about 5 to 10 m.y. after Blake River volcanism, in response to the early stages of regional deformation (D_1) and uplift.

Deformation in the LaRonde Penna Mine Area

Deformation in the Doyon-Bousquet-LaRonde mining camp has been the focus of much attention in the past, owing to the suggestion by many that syntectonic processes played a significant role in the origin of the mineralization and as the mechanism responsible for Au emplacement (e.g., Savoie et al., 1991; Tourigny et al., 1989a, b, 1993; Marquis et al., 1990a, b). As is generally the case for moderately metamorphosed volcanic terranes, the deformation is highly heterogeneous in the study area, with preservation of domains in which primary features are largely undeformed (e.g., Bleeker, 1999) or at least still recognizable. Thus, it has been possible to reconstruct much of the primary geologic setting of the ore lenses at LaRonde Penna, despite the presence of high-strain corridors.

The steep southerly dip of the south-facing homoclinal sequence at LaRonde Penna is attributed to the first regional deformation event (D_1), which is thought to have resulted from collision between the Southern volcanic zone and the Northern volcanic zone of the Abitibi subprovince along the Destor-Porcupine-Manneville fault zone (Hubert et al., 1984; Chown et al., 1992). There are no penetrative structures related to D_1 in the LaRonde Penna area.

Main deformation (D_M)

The main deformation event (D_M), responsible for the formation of the main fabrics developed in the LaRonde Penna area and elsewhere in the Blake River Group, is attributed to D_2 regional deformation (e.g., Hubert et al., 1984). A moderately to strongly developed penetrative schistosity (S_M) is the principal manifestation of D_M. This schistosity trends east-west and dips steeply south (Fig. 9A). It is defined by the relative flattening and/or stretching of markers such as breccia fragments and amygdules (Fig. 10A) and by schistose compositional bands in highly altered rocks. This schistosity S_M is also recognized as centimeter-wide compositional layering within the massive sulfide lenses (Fig. 10B).

A pronounced southwest-plunging stretching lineation (L_S; Fig. 9A) is commonly present in the S_M schistosity plane (Fig. 10C), although oblate flattening is clearly the main manifestation of deformation in some areas underground (Fig. 10D). The overall attitude of the ore lenses (long axes) at LaRonde Penna and elsewhere in the Doyon-Bousquet-LaRonde mining camp is subparallel to this stretching lineation. The combination of flattening and stretching along S_M indicates heterogeneous deformation during progressive north-south shortening accompanied by subvertical extension (e.g., Bell, 1981) as suggested by Marquis et al. (1990b) for the Bousquet 2-Dumagami area. A subhorizontal intersection lineation is locally developed on S_M, especially in strongly altered and foliated rocks. This intersection lineation results from the intersection of an east-west, south-dipping, late S_M crenulation on

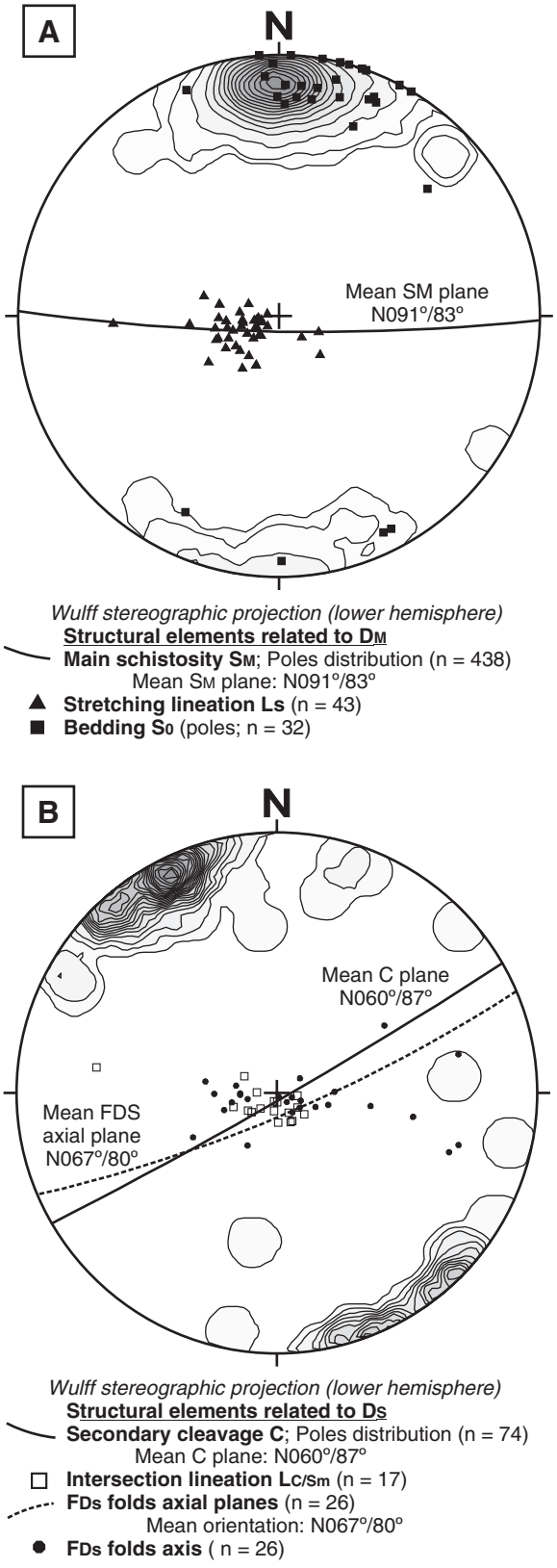

FIG. 9. A. Stereographic projection (Wulff lower hemisphere) of fabrics related to the main deformation event (D_M) that affected the LaRonde Penna ore lenses. B. Stereographic projection (Wulff lower hemisphere) of fabrics related to the secondary deformation event (D_S) that affected the LaRonde Penna ore lenses.

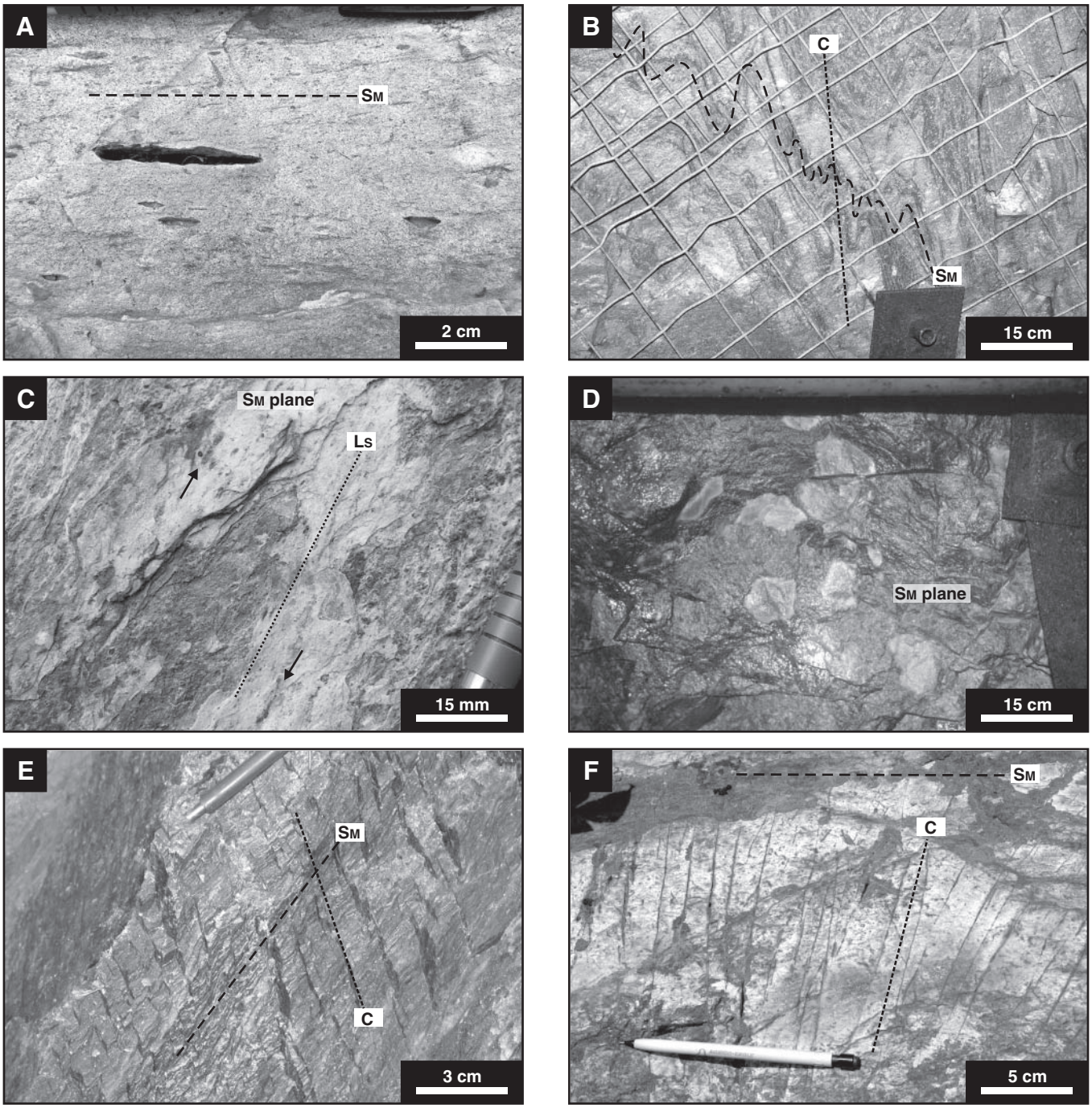

FIG. 10. A. Apparent flattening and stretching on surface (horizontal plane) defining the main schistosity (S_M) oriented east-west and dipping steeply south. B. Example of the main foliation (S_M) defined by millimeter- to centimeter-wide bands of pyrite and sphalerite in massive sulfides of the 20 South lens on level 152 (1,520 m depth). C. Steeply plunging stretching lineation (L_S) developed on the main schistosity (S_M). D. Flattening of fragments of carapace breccia on the main schistosity plane (S_M), suggesting that local oblate deformation occurred after the main (D_M) north-south shortening. E. Example of the east-northeast–west-southwest cleavage (C) related to the secondary deformation event (D_S) that overprints the main foliation (S_M) in ductile graphitic argillite beds within massive sulfides of the 20 South lens on level 106 (1,060 m depth). F. Cleavage-parallel fractures developed within resistant rocks (e.g, rhyolitic breccia fragments) in continuation with the cleavage developed in softer rocks.

the main schistosity plane. It is particularly well developed in the Bousquet and Dumagami mine areas west of LaRonde Penna mine (Tourigny et al., 1989b; Marquis et al., 1990b).

The main deformation event (D_M) was responsible for the generation of decimeter- to meter-wide, east-west–trending, high-strain corridors, mainly near lithological contacts characterized by strong rheological contrasts. Movements along these high-strain corridors are difficult to establish due to reactivations during subsequent deformation events, but a general oblique-dextral movement associated with a minor reverse component can be inferred from different individual strain indicators. Some subvertical, east-west–trending folds (F_{Dm}) exemplified by tightly folded felsic dikes and quartz veins are present. S_M is axial planar to these folds, and the fold axes are colinear with L_S (see below), a phenomenon discussed in detail by Tourigny et al. (1989b) and by Marquis et al. (1990b).

Analysis of these elements shows that the main ductile deformation event (D_M) resulted from north-south to north-northeast–south-southwest subhorizontal compression accompanied by a subvertical extension. The relative flattening and/or stretching of geologic markers attributed to D_M suggests north-south shortening of ~5 times (aspect ratios of 2:1 to 10:1). This interpretation is in agreement with the general tectonic regime related to D_2 in the southeastern Abitibi subprovince (e.g., Dimroth et al., 1983a; Hubert et al., 1984; Daigneault et al., 2002).

Secondary deformation (D_S)

A third period or increment of regional shortening, referred to as the secondary deformation (D_S) at LaRonde Penna, was responsible for development of a subvertical northeast-southwest to east-northeast–west-southwest cleavage (Fig. 9B). This fabric is rarely penetrative and generally forms a millimeter-scale crenulation cleavage developed in previously sericitized rocks and rocks exhibiting the S_M foliation (Fig. 10E). It is also recorded in massive sulfides as alignments of pyrite porphyroblasts, and in the Cadillac Group sedimentary rocks near the contact with the volcanic rocks of the Bousquet Formation. In highly competent rocks, it forms a discrete fracture system in continuity with the cleavage developed in softer rocks (Fig. 10F). The intersection of this subvertical cleavage (C) with the main schistosity (S_M) forms a lineation (L^C_{Sm}) that is steeply plunging to the southwest (Fig. 9B) and colinear with the L_S stretching lineation and the general elongation of the orebodies (Figs. 2B, 4).

Minor folds (F_{Ds}) are associated with the secondary deformation event D_S. These decimeter-scale folds are generally confined to corridors as S_M-intrafolial, S- and sometimes Z-shaped folds in which the axial plane is coplanar to the cleavage (northeast-southwest; Fig. 9B). The F_{Ds} folds are commonly encountered within or close to the ore zones (Fig. 10B), causing thickening of the orebodies and local remobilization of the ore (Mercier-Langevin et al., 2004).

This secondary generation of structures (D_S) is characterized by ductile strain but a late ductile to brittle component is also present, as shown by the common occurrence of a subvertical northeast-southwest and northwest-southeast conjugate fault system. The northeast-southwest faults are recognized throughout the LaRonde Penna area and show limited ($\leq$1 m) sinistral displacements, whereas the northwest-southeast faults show dextral displacements of the same order. Some minor normal to reverse components are locally recorded on these faults, especially near or within the ore zones where it causes minor displacements of the orebodies. These structures indicate that the secondary deformation (D_S) was generated by a north-northwest–south-southeast to north-northeast–south-southwest compression associated with an east-west extension (north-south shortening) where conditions evolved from ductile to ductile-brittle. The D_M and D_S events were collinear, so D_S could be a late expression of D_M instead of a separate deformation event.

Late deformation (D_L)

The late generation of structures (D_L) is manifested by a number of sets of faults, fractures, and veins. The first set comprises shallowly to moderately north- and south-dipping east-west–striking conjugate fractures, faults, and veins. The second set comprises shallowly northwest- and northeast-dipping conjugate fractures and faults and the third set comprises subvertical east-west faults and veins. These late east-west faults represent reactivations of the D_M high-strain corridors and could be an expression of late dextral displacements recognized elsewhere in the South volcanic zone of the Abitibi subprovince (e.g., Daigneault et al., 2002). Some of these late sets of fractures show minor displacements and are filled by quartz and carbonate veins.

In summary, the LaRonde Penna deposit was deformed by a predominantly north-south compression that can be divided into multiple increments (D_1, D_M, D_S, and perhaps D_L, Table 4). The main deformation event at LaRonde Penna (D_M) controls the general attitude of the ore zones and their envelope (flattening, stretching, and some folding). The secondary structures (D_S) control the internal geometry of the ore zones as exemplified by the cleavage, the F_{Ds} small-scale folds, and the conjugate northeast-southwest and northwest-southeast faults. The late deformation had a relatively limited effect on the ore zone geometry.

Synthesis of the LaRonde Penna Mine Stratigraphy and Primary Depositional Setting of the LaRonde-Bousquet 2 Au-Rich VMS Complex

Three schematic stratigraphic columns are presented here to illustrate the overall stratigraphic context and the complex distribution of some units of the upper member of the Bousquet Formation in the LaRonde Penna mine area. The first column (Fig. 11A) corresponds to the stratigraphy at the surface. The second column (Fig. 11B) shows the geology in the upper part of the mine (~850–1,800 m depth). The third column (Fig. 11C) shows the geology of the deeper part of the mine (~1,800–2,300 m depth).

The distribution of the main volcanic units on surface and at different levels underground and the metal distribution within the ore lenses help define two orthogonal synvolcanic fault (or fracture) sets that controlled the emplacement and distribution of the volcanic units (Mercier-Langevin, 2005). The main set corresponds to a depression located along the axis of the LaRonde Penna deposit, and the main volcanic units and ore lenses (LaRonde Penna and Bousquet 2-Dumagami) are elongated along this set of inferred synvolcanic faults (Fig. 12). The second set is more or less perpendicular

TABLE 4. Summary of the Main Fabrics Recognized in the LaRonde Penna Deposit Area

Event	Elements	Description	Distribution	Kinematics	Effects on the ore zones geometry
D_1	S0/S1	Transposed contacts	S0 locally recognized, S1 absent	N-S shortening	South facing homoclinal sequence
D_M (D_2)	S_M (S_2)	Main penetrative schistosity	Main fabric, omnipresent	N-S to NNE-SSW shortening, flattening and stretching (2:1 to 10:1, avg. 5:1)	Flattening of the ore lenses, transposition and tectonic/ metamorphic banding of the sulfides
		Narrow high-strain corridors related to S_M	Mainly near lithological contacts	E-W to NNE-SSW, south dipping, associated to L_S. Subhorizontal striae common	Concentration of strain (S_M) in previously altered and mineralized areas, flattening and possible transposition
	L_S	Mineral and stretching lineation	Near the ore zones and in high-strain zones	Steeply dipping SW on S_M, inferred vertical movement along S_M	Local stretching, perhaps in part responsible for ore shoots
	Lint	Intersection lineation between a N-S subhorizontal cleavage and S_M	Only in high-strain zones, schistose (S_M) rocks	Subhorizontal to shallowly dipping on S_M	None apparent
	P2	Isoclinal folds, cm- to meter-scale	Near lithological contacts	Subvertical hinges, limbs parallel to S_M	Localized stratigraphic repetitions
D_S	C	Secondary cleavage, crenulation and discrete fractures	In S_M-schistosed rocks (cleavage) or silicified rocks (fractures)	NE-SW to ENE-WSW, dipping steeply SE	None apparent
	L^C_{Sm}	Intersection lineation of C on the main schistosity S_M	Within highly altered zones and sedimentary rocks	Steeply dipping SSE to SSW	Possible accentuation of pre-existing ore shoots
	P3	Dm-scale folds (S- and Z-shaped)	In massive sulfide lenses and altered host rocks	E-W to NE-SW, moderately to steeply dipping, intrafolial	Folding of the ore zones with local repetition at small scale
	late D_S faults	Late conjugate fault system	In the ore zones and in the altered host rocks	Subvertical NW-SE (dextral) and NE-SW (senestral) system, minor vertical component	<1 m apparent dextral and senestral offsets of the ore lenses

to the main set and is best illustrated by the metal distribution within the LaRonde Penna ore lenses (Fig. 12). It is suggested that the intersection of these two fault sets created enhanced cross-stratal permeability important for ore-bearing hydrothermal fluids (Mercier-Langevin, 2005).

The units of the upper member of the Bousquet Formation have an irregular distribution across the Doyon-Bousquet-LaRonde mining camp (see Lafrance et al., 2003; Mercier-Langevin et al., 2007b) but are thickest in the LaRonde Penna mine area. A dacitic to rhyodacitic flow breccia (unit 5.1b) marks the transition from large-scale mafic tholeiitic through transitional volcanism to small-scale (flow dome) felsic-dominated transitional to calc-alkaline volcanism (see also Mercier-Langevin et al., 2007a). This dacitic to rhyodacitic flow breccia is intercalated with felsic domes and lobes, andesitic flows, and thin beds of volcanogenic sedimentary rocks and graphitic argillite, and it is cut by mafic sills and dikes. On surface, the andesites form two massive amygdaloidal flows, the first at the base of the unit and the second in the center of the 5.1b unit. This second andesite flow is overlain by fine-grained hyaloclastite. This volcanic architecture suggests a dynamic environment characterized by the emplacement of intermittent felsic autoclastic flows and andesitic flows within restricted depressions where local or intermittent sedimentation occurred prior to burial by felsic volcanic rocks. Zone 6 probably formed during a volcanic hiatus in or near local subbasins as Au-rich massive sulfide clasts are present within the surrounding talus and flow-breccia deposits and volcanogenic sedimentary rocks. Zone 7, at depth, is associated with mafic sills and dikes that acted as impermeable barriers to upward migration of fluid (see also Dubé et al., 2007)

Felsic volcanism continued with the emplacement of unit 5.2b rhyodacitic to rhyolitic flow-breccia deposits and rhyolitic domes or cryptodomes. The first of these domes or cryptodomes is exposed on surface (Figs. 2A, 4, 11A) and can be traced to a depth of about 1,500 m (Figs. 4, 11B). The second appears at a depth of about 2,000 m (Figs. 2B, 4, 11C) and becomes larger at greater depth. This rhyolite is slightly more evolved in terms of geochemistry than the host rhyodacite-rhyolite, which suggests that evolution of the magma chamber was temporally associated with the beginning of the hydrothermal activity responsible for the 20 North and Bousquet 2-Dumagami lenses (see Mercier-Langevin et al., 2007a). The rhyolite domes or cryptodomes were emplaced on top of one of the major faults related to the main fault set (Fig. 12), synchronously with the rhyodacitic to rhyolitic flow breccia deposits that later completely covered the domes or cryptodomes at around 2698.3 ± 0.8 Ma.

A subsequent break in volcanic activity is indicated by the deposition of thin graphitic argillite beds exposed on surface (Fig. 11A) and underground in the upper mine levels (Fig. 11B), and by the formation of Zn-rich massive sulfides on the same horizon as the argillite (20N Zn zone). This represents the earliest expression of the hydrothermal system responsible for formation of the 20 North lens on top of unit 5.2b. On surface and in the upper mine levels, the upper contact of the rhyodacite-rhyolite unit is marked by the feldspar- and quartz-phyric rhyolite (unit 5.3) and the basaltic andesite (unit 5.4) (Figs. 2A, 11A). These two units

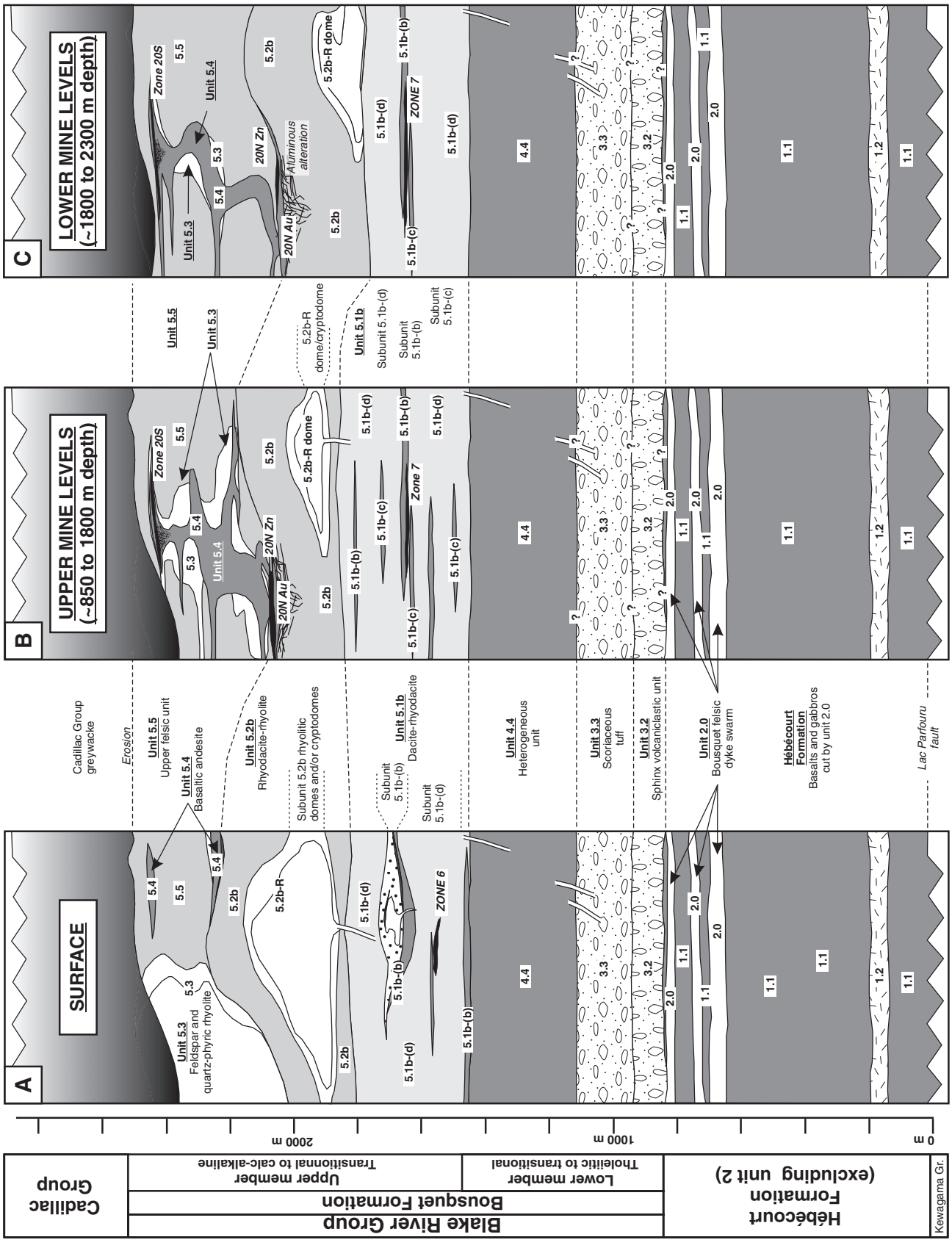

FIG. 11. Composite schematic stratigraphic columns showing the geologic context of different parts of the LaRonde Penna deposit. A. Simplified geology from surface to about 0.8 km below surface. B. Simplified geology of the upper mine levels (from about 0.8 to 1.8 km below surface). C. Simplified geology of the lower mine levels (from about 1.8 to 2.3 km below surface). Scale is approximate.

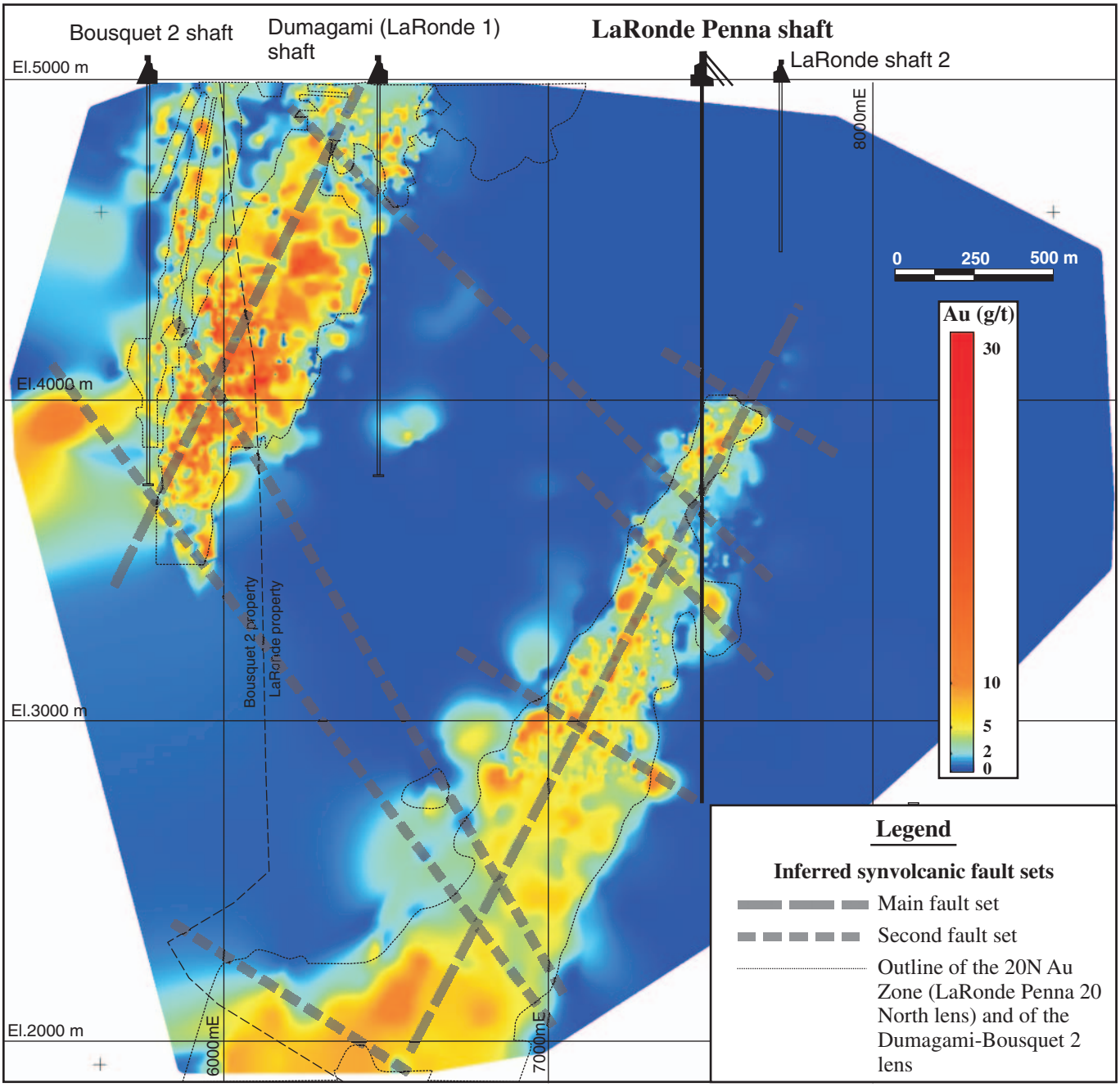

FIG. 12. Longitudinal view (looking north) showing the distribution of the Au within the 20N Au zone (20 North lens) of the LaRonde Penna deposit and of the Dumagami-Bousquet 2 lens. This image of the Au distribution was obtained by the interpolation (simple, natural neighbors) of more than 3500 production drill-hole intersections. High and low Au grade trends were used to constrain the interpreted synvolcanic faults that also partly controlled the volcanic units distribution in this area.

become less important with increasing depth (Figs. 2B, 11C). The feldspar- and quartz-phyric rhyolite is particularly abundant on surface (Fig. 11A) compared to the basaltic andesite, which is more abundant in the Zn-rich part of the deposit (upper mine levels; Figs. 2B, 11B). The distribution and the age of the feldspar- and quartz-phyric rhyolite (unit 5.3) suggest that it was emplaced as a partly extrusive cryptodome on top of unit 5.2b and, in part, within the flow-breccia deposits of unit 5.5 at about 2697.8 ± 1 Ma. Therefore, unit 5.3 volcanism was at least in part coincident with volcanism that produced unit 5.5, as unit 5.3 is hosted by unit 5.5 and fragments of unit 5.3 are present in the upper part of unit 5.5. As for the coherent rhyodacite-rhyolite of unit 5.2b, the feldspar- and quartz-phyric rhyolite of unit 5.3 was characterized by a relatively low permeability (see Dubé et al., 2007) that may have focussed fluids into the underlying permeable footwall rhyodacite-rhyolite (unit 5.2b), resulting in partial replacement of the autoclastic breccias.

As the effusive volcanism responsible for emplacement of the upper felsic unit (unit 5.5) continued, the shallow basaltic andesite sill and dike complex (unit 5.4) was emplaced within unit 5.5, locally cutting through the feldspar- and quartz-phyric rhyolite (Figs. 2B, 11B). The sill and dike complex most probably occupied the same conduits as the porphyritic rhyolite, as suggested by the distribution of both units. A secondary permeability developed as fractures formed in the basaltic andesite during cooling (Dubé et al., 2007), and hydrothermal fluids moved upward to form the 20 South lens higher in the stratigraphy.

The close spatial association of the feldspar- and quartz-phyric rhyolite and the basaltic andesite on top of the 20 North lens likely indicates the presence of synvolcanic faults in this area. This interpretation is supported by the distribution of the two domes or cryptodomes of rhyolite (unit 5.2b) in the 20 North lens footwall and by the stacking of the 20 North and 20 South sulfide lenses. Felsic volcanism was probably active for some time after emplacement of the basaltic andesite (unit 5.4), but the top of the volcanic sequence was eroded and subsequently covered by the Cadillac Group turbidites at least 5 to 10 m.y. after cessation of volcanism, as indicated by the age of the youngest Cadillac Group detrital zircon at LaRonde Penna (2689 Ma). The presence of the unconformity makes it impossible to define the precise timing relationship between volcanism and overlying sedimentation.

Relationships between Geology and Mineralization

The feldspar- and quartz-phyric rhyolite and the basaltic andesite sills and dikes in the hanging wall of the 20 North lens were emplaced within the rhyodacitic to rhyolitic upper felsic unit (5.5) on top of the rhyodacite-rhyolite flow breccia of unit 5.2b, at least partly in a depression generated by the emplacement and growth of the footwall rhyolitic domes or cryptodomes of unit 5.2b (subunit 5.2b-R). The Zn-rich part of the 20 North lens (20N Zn zone) is located in the same depression. In the deeper levels of the mine the 20 North lens is still present, and it is in part located above one of the unit 5.2b footwall rhyolite domes or cryptodomes (Figs. 2B, 4). The distribution of the different alteration facies associated with the Zn-rich massive sulfides in the upper part of the mine versus the aluminous alteration at depth is interpreted to reflect variations in the distribution of the different volcanic units, as illustrated in Figure 13. The gradual transition from base metal-rich ore to Au ± Cu ore and Au ± Cu-Zn ore and aluminous alteration in the 20 North lens horizon at depth could reflect the proximity to the rhyolite dome or cryptodome delineated at depth in the mine (Figs. 2B, 4). The aluminous or advanced argillic alteration developed in this part of the deposit may have resulted from the release of magmatic volatiles by the dome or cryptodome directly to the hydrothermal system very near the ore horizon, which would have acidified the fluids (Sillitoe et al., 1996; Giggenbach, 1997, 2003). The proximity of an effusive felsic center also indicates the presence of conduits that may have channelled magmatic fluids high in the volcanic sequence from a shallow magma chamber (cf. "crack zone" of de Ronde et al., 2005).

The LaRonde Penna deposit environment is characterized by a thickening of the upper member of the Bousquet Formation, including a local felsic-dominated volcanic center (Lafrance et al., 2003) composed of discrete elongate felsic flow-dome complexes and mafic sill and dike swarms located above synvolcanic faults. This volcanic center could have been part of a larger composite volcano and/or caldera complex, as documented in many active submarine arc volcanoes (e.g., Kermadec and Izu-Bonin arcs; Fiske et al., 2001; Wright et al., 2002; de Ronde et al., 2005).

The different alteration and mineralization styles at LaRonde Penna are best explained by variations along strike in the style of volcanism and magmatic activity, with dominantly

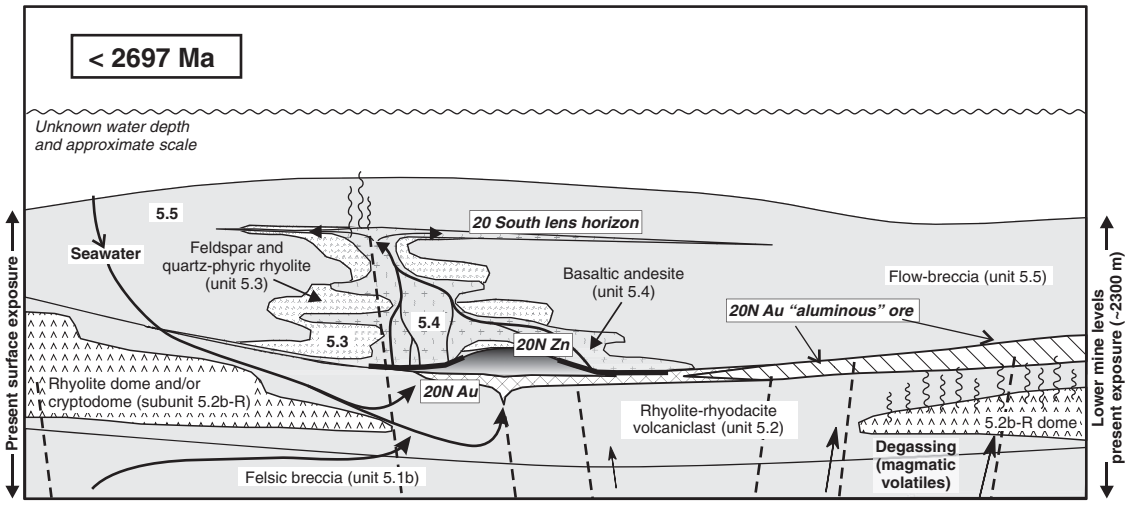

FIG. 13. Schematic representation (not to scale) of the distribution of the main units of the upper member of the Bousquet Formation in the LaRonde Penna deposit area prior to deformation. The variations in ore and alteration style observed along the ore lenses at depth, especially along the 20 North lens, are illustrated. A period of localized transitional to calc-alkaline felsic volcanism (domes, cryptodomes, and flow-breccia deposits of units 5.1b and 5.2b) marks the magmatic evolution from regional tholeiitic to transitional, mafic-dominated volcanism (effusive and explosive; lower member of the Bousquet Formation). This shift in magmatic activity is coincident with the initiation of the hydrothermal activity responsible for the formation of the stacked Au-rich lenses of the LaRonde Penna deposit. See text for discussion.

quartz-biotite-garnet-muscovite propylitic alteration and Au-Zn-Cu-Ag-Pb mineralization (caused by near-neutral hydrothermal fluids) in the volcaniclastic units in the upper levels of the mine (Dubé et al., 2007), and advanced argillic alteration and Au-Cu mineralization (caused by acidic fluids; Dubé et al., 2007) proximal to shallow felsic subvolcanic intrusions or cryptodomes at greater depth in the mine. This situation contrasts with many subaerial volcanic centers in which near-neutral and intensely acid conditions, unless telescoped, commonly occur in temporally, as well as spatially, separate volcanic-hydrothermal systems. It also contrasts with the proposed model for high-sulfidation deposits formed in the VMS environment where low-sulfidation and high-sulfidation conditions are thought to develop at very different positions relative to a submarine felsic dome complex (Sillitoe et al., 1996). However, these different conditions also appear to be possible in different parts of the same hydrothermal system, in large part due to variable degrees of mixing of magmatic volatile-rich fluids and hydrothermally convected seawater (Fig. 14). The model proposed here for the LaRonde Penna deposit is supported by the gradual transition between the two ore styles in the 20 North lens and the formation of the aluminous zone by subsea-floor replacement (Dubé et al., 2007). In this empirical model, magma degassing is enhanced at shallow depth in a volcanic complex (e.g., rhyolitic domes or cryptodomes) and channelled into crack zones, whereas magma emplaced at greater depth may result in larger hydrothermal cells and greater involvement of seawater and enhanced water-rock interaction (Giggenbach, 1997; Hannington et al., 1999). Strongly acidic hydrothermal solutions can only be generated from high-temperature magmatic fluids, and the acids are likely to be neutralized at intermediate depth and temperature (Giggenbach, 2003). This likely explains the location of the aluminous alteration at LaRonde Penna above a felsic dome or cryptodome complex. Similar variations are observed in the active submarine hydrothermal system of the Brothers Volcano on the Kermadec arc, New Zealand, where sulfide chimneys and hydrothermal plumes are associated with the localized venting of acidic magmatic fluids between and on top of felsic domes emplaced within a caldera (de Ronde et al., 2005). This demonstrates that the proximity of the deposits relative to the source (or conduits) of magmatic fluids has a major impact on the style of alteration and mineralization in a VMS environment.

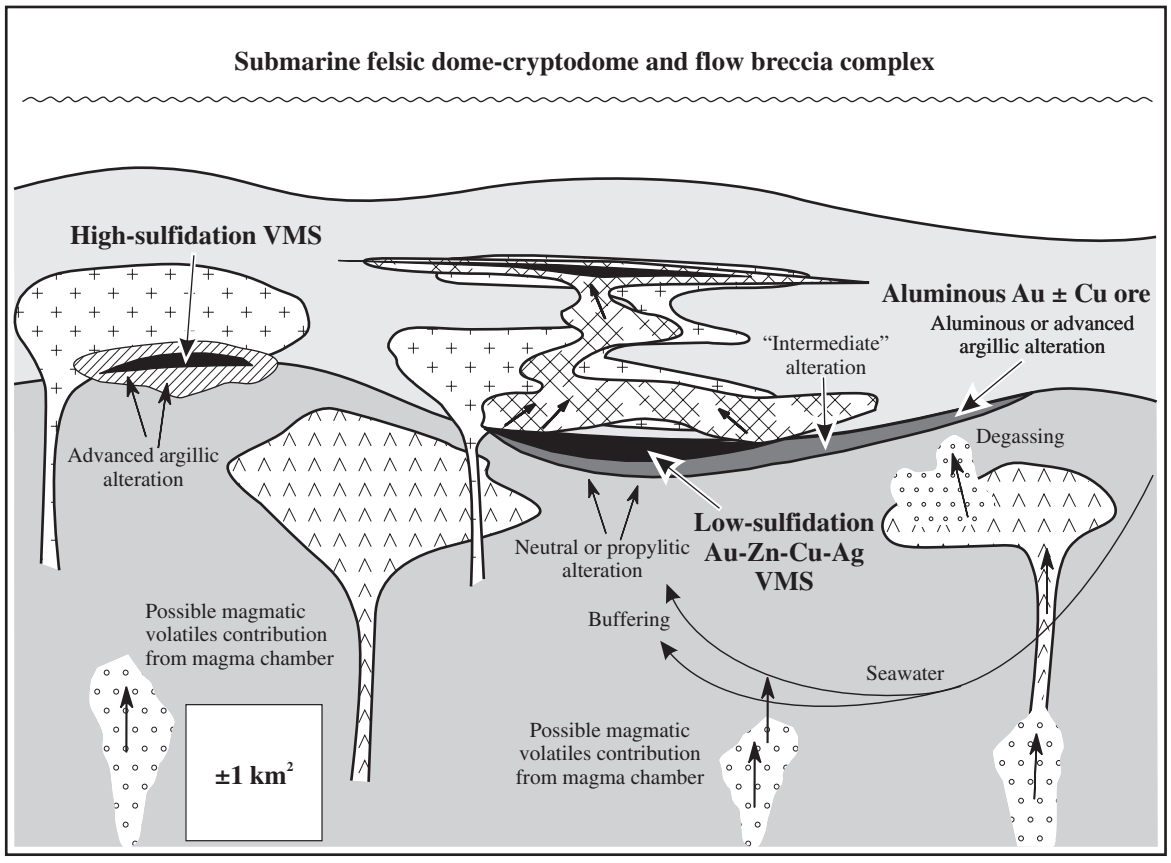

FIG. 14. Schematic section that illustrates the favorable environment for high- and low-sulfidation VMS lenses in a submarine felsic dome-cryptodome and flow breccia complex from the simplified volcanic architecture of the host sequence of the LaRonde-Bousquet 2 Au-rich VMS complex. The proposed model is a modified version of that presented by Sillitoe et al. (1996). It shows that a VMS system can generate mineralization styles that gradually evolve (spatially and temporally) from neutral Au-Cu-Zn-Ag-Pb ore, to transitional, to acidic advanced argillic alteration and Au ± Cu ore in response to the evolving local geologic context. In this model, the ore type is not controlled by the water depth but rather by a variable contribution of seawater and magmatic volatiles (degassing) to the mineralizing fluids that is then variably buffered and transports different metal assemblages.

Based on the reconstruction of the volcanic facies at LaRonde Penna and comparison with other VMS systems, shallow magma (subvolcanic intrusions) emplaced within the volcanic pile might have contributed directly to the hydrothermal system, producing advanced argillic alteration associated with Au ± Cu ore, whereas the seawater-dominated portion of the system produced the Zn-rich part of the LaRonde Penna deposit. Synvolcanic faulting near the Zn-rich part of the deposit also may have caused enhanced permeability and incursion of larger volumes of seawater (Fig. 14). The relative contribution of magmatic volatiles in different parts of the system may also reflect the depth of the subvolcanic intrusions. For example, the Mooshla composite synvolcanic intrusion, about 7 km west of LaRonde Penna (Fig. 1), hosts syngenetic Au-Cu veins and disseminations associated with aluminous alteration that extends eastward, outside the intrusion into the volcanic sequence (Galley and Lafrance, 2007). The intrusion-related mineralized system is associated with the late, calc-alkaline, volatile-rich intrusive phases of the Mooshla pluton and has some similarities to epithermal-style mineralization (Galley and Lafrance, 2007). The Moohsla intrusion could, therefore, be the source of the inferred magmatic component in the LaRonde Penna Au-rich VMS deposit hydrothermal system, which is of the same age but located higher in the stratigraphy. When compared to other intrusion-related VMS camps, the Mooshla intrusion seems to be too small to be the heat engine for the generation of the VMS deposits of the camp (cf. Galley, 2003). However, the presence of this composite and volatile-rich intrusion at a high stratigraphic level is evidence for important high-level felsic magmatic conduits in this area.

Summary and Conclusions

Despite the superposition of late tectonic and metamorphic events, the primary geologic characteristics of the LaRonde Penna Au-rich VMS deposit are sufficiently well preserved to allow detailed description and reconstruction of the primary setting of mineralization. The key geologic parameters that controlled the formation of the LaRonde Penna deposit and its various ore and alteration styles include the intermediate (andesite) to felsic (dacite, rhyodacite, and rhyolite), transitional to calc-alkaline effusive volcanism and shallow intrusions that formed a complex of permeable autoclastic deposits cut and overlain by less permeable domes, cryptodomes, sills, and dikes. These features were associated with the development of volcanic vents and depressions focussing hydrothermal fluid circulation.

The magmatic evolution of the volcanic complex is characterized by tholeiitic to transitional, mafic to felsic rocks at the base (north), and transitional to calc-alkaline, intermediate to felsic rocks on top (south), defining a continuous magmatic trend, rather than a bimodal volcanic sequence. This differs from the mine sequence of the Noranda Volcanic Complex, about 50 km to the west, in which the VMS-hosting volcanic rocks are mainly bimodal and largely dominated by mafic to intermediate basalt and andesite (Gélinas and Ludden, 1984; Gélinas et al., 1984). The Hébécourt Formation and lower member of the Bousquet Formation comprise a thick substratum on which the intermediate to felsic volcanic rocks of the upper member were emplaced as restricted coalescent domes or cryptodomes at submarine effusive centers. These rocks host the LaRonde Penna and the neighboring Bousquet 2-Dumagami and Bousquet deposits, and local subbasins between the domes or cryptodomes appear to have been the locus of much of the sulfide accumulation. Volcanic features of the locally thickened Bousquet formation near LaRonde Penna (e.g., permeable units cut by impermeable units) helped focus hydrothermal upflow and contributed to efficient metal deposition. Active volcanism within the relatively restricted setting of the LaRonde Penna deposit and rapid burial of the host sequence likely contributed to the large size of the massive sulfide lenses, with the deposits growing partly by subsea-floor replacement of the permeable footwall breccias.

The hydrothermal activity was characterized by variable contributions of magmatic volatiles and convective hydrothermal circulation of seawater within a single, protracted system. It is proposed here that different styles of alteration and mineralization along strike are related to the relative contributions of magmatic volatiles and hydrothermal seawater. The strong permeability contrasts that resulted from autoclastic, flow-breccia deposits being cut by and buried by less permeable felsic domes or cryptodomes and intermediate to mafic sills and dikes determined the hydrologic regime. The emplacement of a relatively impermeable feldspar- and quartz-phyric rhyolite cryptodome above the 20 North lens enhanced subsea-floor replacement of the footwall felsic breccia by the ore, and a shallowly emplaced mafic sill and dike complex above the 20 North lens also helped to focus hydrothermal fluids through fractures into the overlying 20 South lens.

The formation of the LaRonde Penna deposit at ca. 2698 Ma corresponds to a particularly fertile episode of Au-rich VMS formation in the Blake River Group. The host rocks of the deposit are among the youngest dated units in the Blake River Group, suggesting a possible correlation between the petrogenetic evolution of this volcanic assemblage and the enrichment of Au in the VMS (see Mercier-Langevin et al., 2007a). Deformation and metamorphism greatly modified the primary hydrothermal assemblages and the alteration but were not responsible for the introduction of Au, as previously proposed for other deposits of the district. The early, synvolcanic introduction of Au is supported by a number of observations from the ore zones and the alteration zones, as discussed in Dubé et al. (2007), as well as a number of other features of the mine sequence stratigraphy presented in this study. These include the following: (1) the presence of Au-rich clasts in some volcanic breccias near zone 6, (2) stacking of discrete Au-rich lenses within the volcanic succession, with little or no Au mineralization between the lenses, (3) the preserved primary distribution of Au and Cu in the highly strained lenses along synvolcanic faults, and (4) the correlation of different volcanic facies with Au enrichment. At LaRonde Penna, the presence of sulfide lenses characterized by Au-rich portions and base metal-rich portions (e.g., 20 North lens) demonstrates that mineralization styles gradually evolved (spatially and temporally) from neutral (Au-Cu-Zn-Ag-Pb ore), to transitional, to acidic (advanced argillic alteration and Au ± Cu-rich ore) conditions in response to the evolving local geologic context.

Acknowledgments

The authors wish to express their sincere appreciation to Agnico-Eagle Mines Ltd. and the LaRonde Penna mine geology department staff for financial and logistical support and for an essential scientific contribution, critical review, and authorization to publish. We are grateful to the Ministère des Ressources Naturelles, de la Faune et des Parcs du Québec for support in this project, and for a great input by J. Moorhead and P. Pilote to the Doyon-Bousquet-LaRonde synthesis. Special thanks to the staff at Barrick's Bousquet 2 mine and Cambior's Doyon and Mouska mines for sharing their knowledge of the district. We especially thank A. Galley, J. Franklin, H.K. Poulsen, M. Richer-Laflèche, H. Gibson, F. Chartrand, M. Rocheleau, W. Mueller, R. Daigneault, D. Gaboury, and A. Fowler for constructive discussions in the field and valuable scientific input. C. Deblonde, P. Brouillette, H. Julien, and L. Dubé contributed to the construction of the database and the drawing of some figures. The first author (P. Mercier-Langevin) would like to acknowledge the SEG Canada Foundation, NSERC, INRS-ETE, and FCAR for providing grant scholarships. D.W.D. acknowledges NSERC MFA support for maintenance of the geochronology laboratory. This paper was substantially improved by helpful comments by A. Galley and G. Long, and by constructive reviews by S. Scott, C.T. Barrie, and K. Kelley.

REFERENCES

Ayer, J., Amelin, Y., Corfu, F., Kamo, S., Ketchum, J., Kwok, K., and Trowell, N., 2002, Evolution of the southern Abitibi greenstone belt based on U-Pb geochronology: Autochtonous volcanic construction followed by plutonism, regional deformation and sedimentation: Precambrian Research, v. 115, p. 63–95.

Barrie, C.T., and Hannington, M.D., 1999, Classification of volcanic-associated massive sulphide deposits based on host-rock composition: Reviews in Economic Geology, v. 8, p. 1–11.

Barrie, C.T., Ludden, J.N., and Green, T.H., 1993, Geochemistry of volcanic rocks associated with Cu-Zn and Ni-Cu deposits in the Abitibi subprovince: Economic Geology, v. 88, p. 1341–1358.

Belkabir, A., and Hubert, C., 1995, Geology and structure of a sulfide-rich gold deposit: An example from the Mouska gold mine, Bousquet district, Canada: Economic Geology, v. 90, p. 1064–1079.

Bell, T.H., 1981, Foliation development—the contribution, geometry and significance of progressive, bulk, inhomogeneous shortening: Tectonophysics, v. 75, p. 273–296.

Bleeker, W., 1999, Structure, stratigraphy, and primary setting of the Kidd Creek volcanogenic massive sulfide deposit: A semiquantitative reconstruction: Economic Geology Monograph 10, p. 71–122.

Bleeker, W., Parrish, R.R., and Sager-Kinsman, A., 1999, High-precision U-Pb geochronology of the Late Archean Kidd Creek deposit and Kidd volcanic complex: Economic Geology Monograph 10, p. 43–70.

Branney, M.J., and Suthren, R.J., 1988, High-level peperitic sills in the English Lake District: Distinction from block lavas, and implications for Borrowdale Volcanic Group stratigraphy: Geological Journal, v. 23, p. 171–187.

Chown, E.H., Daigneault, R., Mueller, W., and Mortensen, J.K., 1992, Tectonic evolution of the Northern volcanic zone, Abitibi belt, Quebec: Canadian Journal of Earth Sciences, v. 29, p. 2211–2225.

Corfu, F., 1993, The evolution of the southern Abitibi greenstone belt in light of precise U-Pb geochronology: Economic Geology, v. 88, p. 1323–1340.

Corfu, F., Krogh, T.E., Kwok, Y.Y., and Jensen, L.S., 1989, U-Pb zircon geochronology in the southwestern Abitibi greenstone belt, Superior province: Canadian Journal of Earth Sciences, v. 26, p. 1747–1763.

Daigneault, R., Mueller, W.U., and Chown, E.H., 2002, Oblique Archean subduction: Accretion and exhumation of an oceanic arc during dextral transpression, Southern volcanic zone, Abitibi subprovince Canada: Precambrian Research, v. 115, p. 261–290.

Davis, D.W., 1982, Optimum linear regression and error estimation applied to U-Pb data: Canadian Journal of Earth Sciences, v. 19, p. 2141–2149.

——2002, U-Pb geochronology of Archean metasedimentary rocks in the Pontiac and Abitibi subprovinces, Quebec: Constraints on timing, provenance and regional tectonics: Precambrian Research, v. 115, p. 97–117.

Davis, D.W., and Lin, S., 2003, Unraveling the geologic history of the Hemlo Archean gold deposit, Superior Province, Canada: A U-Pb geochronological study: Economic Geology, v. 98, p. 51–67.

de Ronde, C.E.J., Hannington, M.D., Stoffers, P., Wright, I.C., Ditchburn, R.G., Reyes, A.G., Baker, E.T., Massoth, G.J., Lupton, J.E., Walker, S.L., Greene, R.R., Soong, C.W.R., Ishibashi, J., Lebon, G.T., Bray, C.J., and Resing, J.A., 2005, Evolution of a submarine magmatic-hydrothermal system: Brothers volcano, Southern Kermadec Arc, New Zealand: Economic Geology, v. 100, p. 1097–1133.

Dimroth, E., Imreh, L., Rocheleau, M., and Goulet, N., 1982, Evolution of the south-central part of the Archean Abitibi belt, Quebec. Part I: Stratigraphy and paleogeographic model: Canadian Journal of Earth Sciences, v. 19, p. 1729–1758.

Dimroth, E., Imreh, L., Goulet, N., and Rocheleau, M., 1983a, Evolution of the south-central part of the Archean Abitibi belt, Quebec. Part II: Tectonic evolution and geomechanical model: Canadian Journal of Earth Sciences, v. 20, p. 1355–1373.

——1983b, Evolution of the south-central part of the Archean Abitibi belt, Quebec. Part III: Plutonic and metamorphic evolution and geotectonic model: Canadian Journal of Earth Sciences, v. 20, p. 1374–1388.

Dubé, B., Mercier-Langevin, P., Hannington, M., Davis, D., and Lafrance, B., 2004, Le gisement de sulfures massifs aurifères volcanogènes LaRonde, Abitibi, Québec: Altérations, minéralisations et implications pour l'exploration: Ministère des Ressources naturelles, de la Faune et des Parcs du Québec, MB 2004-03, 112 p.

Dubé, B., Mercier-Langevin, P., Hannington, M.D., Lafrance, B., Gosselin, P., and Gosselin, G., 2007, The LaRonde Penna world-class Au-rich volcanogenic massive sulfide deposit, Abitibi, Quebec: Mineralogy and geochemistry of alteration and implications for genesis and exploration: Economic Geology, v. 102, p. 633–666.

Fiske, R.S., Nada, J., Iizasa, K., Yuasa, M., and Klaus, A., 2001, Submarine silicic caldera at the front of the Izu-Bonin arc, Japan; voluminous seafloor eruptions of rhyolite pumice: Geological Society of America Bulletin, v. 113, p. 813–824.

Galley, A.G., 2003, Composite synvolcanic intrusions associated with Precambrian VMS-related hydrothermal systems: Mineralium Deposita, v. 38, p. 443–473.

Galley, A.G., and Lafrance, B., 2007, Évolution et métallogénie du pluton de Mooshla: Ministère des Ressources naturelles et de la Faune, ET 2007-02, 31 p.

Gélinas, L., and Ludden, J.N., 1984, Rhyolitic volcanism and the geochemical evolution of an Archaean central ring complex: The Blake River Group volcanics of the southern Abitibi belt, Superior Province: Physics of the Earth and Planetary Interiors, v. 35, p. 77–88.

Gélinas, L., Trudel, P., and Hubert, C., 1984, Chemostratigraphic division of the Blake River Group, Rouyn-Noranda area, Abitibi, Quebec: Canadian Journal of Earth Sciences, v. 21, p. 220–231.

Gifkin, C.C., and Allen, R.L., 2001, Textural and chemical characteristics of diagenetic and hydrothermal alteration in glassy volcanic rocks: Examples from the Mount Read Volcanics, Tasmania: Economic Geology, v. 96, p. 973–1002.

Giggenbach, W.F., 1997, The origin and evolution of fluids in magmatic-hydrothermal systems, *in* Barnes, H.L., ed., Geochemistry of hydrothermal ore deposits: 3rd edition: New York, Wiley-Interscience, p. 737–796.

Giggenbach, W.F., 2003, Magma degassing and mineral deposition in hydrothermal systems along convergent plate boundaries [reprint]: Society of Economic Geologists Special Publication Number 10, p. 1–18.

Gosselin, G., 1998, Veines de quartz aurifères précoces à la zone ouest de la mine Doyon, Canton de Bousquet, Preissac, Abitibi: Unpublished M.Sc. thesis, Université du Québec à Chicoutimi, 125 p.

Goto, Y., and McPhie, J., 1998, Endogenous growth of a Miocene submarine dacite cryptodome, Rebun Island, Hokkaido, Japan: Journal of Volcanology and Geothermal Research, v. 84, p. 273–286.

Hanes, J.A., Archibald, D.A., Queen, M., and Farrar, E., 1994, Constraints from $^{40}Ar/^{39}Ar$ geochronology on the tectonothermal history of the Kapuskasing uplift in the Canadian Superior province: Canadian Journal of Earth Sciences, v. 31, p. 1146–1171.

Hannington, M.D., and Scott, S.D., 1989, Gold mineralization in volcanogenic massive sulfides: Implications of data from active hydrothermal vents on the modern sea floor: Economic Geology Monograph 6, p. 491–507.

Hannington, M.D., Poulsen, K.H., Thompson, J.F.H., and Sillitoe, R.H., 1999, Volcanogenic gold in the massive sulfide environment: Reviews in Economic Geology, v. 8, p. 325–356.

Hubert, C., Trudel, P., and Gélinas, L., 1984, Archean wrench-fault tectonics and structural evolution of the Blake River Group, Abitibi belt, Quebec: Canadian Journal of Earth Sciences,v. 21, p. 1024–1032.

Huston, D.L., 2000, Gold in volcanic-hosted massive sulfide deposits: distribution, genesis, and exploration: Reviews in Economic Geology, v. 13, p. 400–426.

Huston, D.L., Bottrill, R.S., Creelman, R.A., Zaw, K., Ramsden, T.R., Rand, S.W., Gemmell, J.B., Jablonski, W., Sie, S.H., and Large, R.R., 1992, Geologic and geochemical controls on the mineralogy and grain size of gold-bearing phases, Eastern Australian volcanic-hosted massive sulfide deposits: Economic Geology, v. 87, p. 542–563.

Huston, D.L., and Large, R.R., 1989, A chemical model for the concentration of gold in volcanogenic massive sulphide deposits: Ore Geology Reviews, v. 4, p. 171–200.

Jaffey, A.H., Flynn, K.F., Glendenin, L.E., Bentley, W.C., and Essling, A.M., 1971, Precision measurement of half-lives and specific activities of ^{235}U and ^{238}U: Physical Review, v. 4, p. 1889–1906.

Jemielita, R.A., Davis, D.W., and Krogh, T.E., 1990, U-Pb evidence for Abitibi gold mineralization postdating greenstone magmatism and metamorphism: Nature, v. 346, p. 831–834.

Lafrance, B., Moorhead, J., and Davis, D., 2003, Cadre géologique du camp minier de Doyon-Bousquet-LaRonde: Ministère des Ressources naturelles, de la Faune et des Parcs du Québec, ET 2002-07, 43 p.

Lafrance, B., Davis, D.W., Goutier, J., Moorhead, J., Pilote, P., Mercier-Langevin, P., Dubé, B., Galley, A., and Mueller, W.U., 2005, Nouvelles datations isotopiques dans la portion québécoise du Groupe de Blake River et des unités adjacentes: Ministère des Ressources naturelles, de la Faune et des Parcs du Québec, RP 2005-01, 15 p.

Lajoie, J., and Ludden, J., 1984, Petrology of the Archean Pontiac and Kewagama sediments and implications for the stratigraphy of the southern Abitibi belt: Canadian Journal of Earth Sciences, v. 21, p. 1305–1314.

Large, R.R., 1992, Australian volcanic-hosted massive sulfide deposits: Features, styles, and genetic models: Economic Geology, v. 87, p. 471–510.

Marquis, P., Brown, A.C., Hubert, C., and Rigg, D.M., 1990a, Progressive alteration associated with auriferous massive sulfide bodies at the Dumagami mine, Abitibi greenstone belt, Quebec: Economic Geology, v. 85, p. 746–764.

Marquis, P., Hubert, C., Brown, A.C., and Rigg, D.M., 1990b, Overprinting of early, redistributed Fe and Pb-Zn mineralization by late-stage Au-Ag-Cu deposition at the Dumagami mine, Bousquet district, Abitibi, Quebec: Canadian Journal of Earth Sciences, v. 27, p. 1651–1671.

McBirney, A.R., 1963, Factors governing the nature of submarine volcanism: Bulletin de Volcanologie, v. 26, p. 455–469.

McPhie, J., and Allen, R.L., 1992, Facies architecture of mineralized submarine volcanic sequences: Cambrian Mount Read Volcanics, Tasmania: Economic Geology, v. 87, p. 587–596.

McPhie, J., Doyle, M., and Allen, R., 1993, Volcanic textures—a guide to the interpretation of textures in volcanic rocks: Centre for Ore Deposit and Exploration Studies, University of Tasmania, 198 p.

Mercier-Langevin, P., 2005, Géologie du gisement de sulfures massifs volcanogènes aurifères LaRonde, Abitibi, Québec: Unpublished Ph.D. thesis, Institut national de la recherche scientifique, Eau, Terre et Environnement, 694 p.

Mercier-Langevin, P., Dubé, B., Hannington, M.D., Davis, D.W., and Lafrance, B., 2004, Contexte géologique et structural des sulfures massifs volcanogènes aurifères du gisement LaRonde, Abitibi: Ministère des ressources naturelles, de la Faune et des Parcs du Québec, ET 2003-03, 47 p.

Mercier-Langevin, P., Dubé, B., Hannington, M.D., Richer-Laflèche, M., and Gosselin, G., 2007a, The LaRonde Penna Au-rich volcanogenic massive sulfide deposit, Abitibi greenstone belt, Quebec: Part II. Lithogeochemistry and paleotectonic setting: Economic Geology, v. 102, p. 611–631.

Mercier-Langevin, P., Dubé, B., Lafrance, B., Hannington, M.D., Galley, A., and Moorhead, J., 2007b, A group of papers devoted to the LaRonde Penna Au-rich volcanogenic massive sulfide deposit, eastern Blake River Group, Abitibi greenstone belt, Quebec—Preface: Economic Geology, v. 102, p. 577–583.

Mortensen, J.K., 1993, U-Pb geochronology of the eastern Abitibi Subprovince. Part 2: Noranda-Kirkland Lake area: Canadian Journal of Earth Sciences, v. 30, p. 29–41.

Mueller, W.U., and Mortensen, J.K., 2002, Age constraints and characteristics of subaqueous volcanic contruction, the Archean Hunter Mine Group, Abitibi greenstone belt: Precambrian Research, v. 115, p. 119–152.

Peloquin, A.S., Potvin, R., Laflèche, M.R., Verpaelst, P., and Gibson, H.L., 1990, The Blake River Group, Rouyn-Noranda area, Quebec: A stratigraphic synthesis, *in* Rive, M., Verpaelst, P., Gagnon, Y., Lulin, J.-M., Riverin, G., and Simard, A., eds., The northwestern Quebec polymetallic belt: A summary of 60 years of mining exploration, CIM Special Volume 43, p. 107–118.

Poulsen, K.H., and Hannington, M.D., 1995, Volcanic-associated massive sulfide gold: Geological Survey of Canada, Geology of Canada, no. 8, The Geology of North America v. P-1, p. 183–196.

Powell, W.G., Carmichael, D.M., and Hodgson, C.J., 1995a, Conditions and timing of metamorphism in the southern Abitibi greenstone belt, Quebec: Canadian Journal of Earth Sciences, v. 32, p. 787–805.

Powell, W.G., Hodgson, C.J., Hanes, J.A., Carmichael, D.M., McBride, S., and Farrar, E., 1995b, $^{40}Ar/^{39}Ar$ geochronological evidence for multiple hydrothermal events focused along faults in the southern Abitibi greenstone belt: Canadian Journal of Earth Sciences, v. 32, p. 768–786.

Savoie, A., Trudel, P., Sauvé., P., Hoy, L., and Lao, K., 1991, Géologie de la mine Doyon (région de Cadillac): Ministère des ressources naturelles du Québec, ET 90-05, 80 p.

Sillitoe, R.H., Hannington, M.D., and Thompson, J.F.H., 1996, High sulfidation deposits in the volcanogenic massive sulfide environment: Economic Geology, v. 91, p. 204–212.

Stone, W.E., 1990, Archean volcanism and sedimentation in the Bousquet gold district, Abitibi greenstone belt, Quebec: Implications for stratigraphy and gold concentration: Geological Society of America Bulletin, v. 102, p. 147–158.

Tourigny, G., Hubert, C., Brown, A.C., and Crépeau, R., 1988, Structural geology of the Blake River at the Bousquet mine, Abitibi, Quebec: Canadian Journal of Earth Sciences, v. 25, p. 581–592.

Tourigny, G., Brown, A.C., Hubert, C., and Crépeau, R., 1989a, Synvolcanic and syntectonic gold mineralization at the Bousquet mine, Abitibi greenstone belt, Quebec: Economic Geology, v. 84, p. 1875–1890.

Tourigny, G., Hubert, C., Brown, A.C., and Crépeau, R., 1989b, Structural control on gold mineralization at the Bousquet mine, Abitibi, Quebec: Canadian Journal of Earth Sciences, v. 26, p. 157–175.

Tourigny, G., Doucet, D., and Bourget, A., 1993, Geology of the Bousquet 2 mine: An example of a deformed, gold-bearing polymetallic sulfide deposit: Economic Geology, v. 88, p. 1578–1597.

Valliant, R.I., and Hutchinson, R.W., 1982, Stratigraphic distribution and genesis of gold deposits, Bousquet region, Northwestern Quebec, *in* Hodder, R.W., and Petruk, W., eds., Geology of Canadian gold deposits: CIM Special Volume 24, p. 27–40.

Vervoot, J.D., White, W.M., Thorpe, R.I., and Franklin, J.M., 1993, Postmagmatic thermal activity in the Abitibi greenstone belt, Noranda and Matagami districts: Evidence from whole-rock Pb isotopic data: Economic Geology, v. 88, p. 1598–1614.

Wright, I.C., Stoffers, P., Hannington, M., de Ronde, C.E.J., Herzig, P., Smith, I.E.M., and Browne, P., 2002, Towed-camera investigations of shallow-intermediate water depth submarine basaltic stratovolcanoes of the southern Kermadec arc: Marine Geology, v. 185, p. 207–218.

Wyman, D.A., Kerrich, R., and Polat, A., 2002, Assembly of Archean cratonic mantle lithosphere and crust: Plume-arc interaction in the Abitibi-Wawa subduction-accretion complex: Precambrian Research, v. 115, p. 37–62.